UDP-glucuronosyltransferases encoded at the UGT1 locus. Biochem Biophys Res Commun 260:199–202
6. Gagne JF, Montminy V, Belanger P, Journault K, Gaucher G, Guillemette C (2002) Common human UGT1A polymorphisms and the altered metabolism of irinotecan active metabolite 7-ethyl-10-hydroxycamptothecin (SN-38). Mol Pharmacol 62:608–617
7. Hanioka N, Ozawa S, Jinno H, Ando M, Saito Y, Sawada J (2001) Human liver UDP-glucuronosyltransferase isoforms involved in the glucuronidation of 7-ethyl-10-hydroxycamptothecin. Xenobiotica 31:687–699
8. Ritter JK, Chen F, Sheen YY, Tran HM, Kimura S, Yeatman MT, Owens IS (1992) A novel complex locus *UGT1* encodes human bilirubin, phenol, and other UDP-glucuronosyltransferase isozymes with identical carboxyl termini. J Biol Chem 267:3257–3261
9. Zheng Z, Park JY, Guillemette C, Schantz SP, Lazarus P (2001) Tobacco carcinogen-detoxifying enzyme UGT1A7 and its association with orolaryngeal cancer risk. J Natl Cancer Inst 93:1411–1418
10. Strassburg CP, Strassburg A, Nguyen N, Li Q, Manns MP, Tukey RH (1999) Regulation and function of family 1 and family 2 UDP-glucuronosyltransferase genes (UGT1A, UGT2B) in human oesophagus. Biochem J 338:489–498
11. Strassburg CP, Nguyen N, Manns MP, Tukey RH (1998) Polymorphic expression of the UDP-glucuronosyltransferase UGT1A gene locus in human gastric epithelium. Mol Pharmacol 54:647–654
12. Ockenga J, Vogel A, Teich N, Keim V, Manns MP, Strassburg CP (2003) UDP glucuronosyltransferase (UGT1A7) gene polymorphisms increase the risk of chronic pancreatitis and pancreatic cancer. Gastroenterology 124:1802–1808
13. Strassburg CP, Manns MP, Tukey RH (1998) Expression of the UDP-glucuronosyltransferase 1A locus in human colon. Identification and characterization of the novel extrahepatic UGT1A8. J Biol Chem 273:8719–8726
14. Villeneuve L, Girard H, Fortier LC, Gagne JF, Guillemette C (2003) Novel functional polymorphisms in the UGT1A7 and UGT1A9 glucuronidating enzymes in Caucasian and African-American subjects and their impact on the metabolism of 7-ethyl-10-hydroxycamptothecin and flavopiridol anticancer drugs. J Pharmacol Exp Ther 307:117–128
15. Jinno H, Saeki M, Saito Y, Tanaka-Kagawa T, Hanioka N, Sai K, Kaniwa N, Ando M, Shirao K, Minami H, Ohtsu A, Yoshida T, Saijo N, Ozawa S, Sawada J (2003) Functional characterization of human UDP-glucuronosyltransferase 1A9 variant, D256N, found in Japanese cancer patients. J Pharmacol Exp Ther 306:688–693
16. Lankisch TO, Vogel A, Eilermann S, Fiebeler A, Krone B, Barut A, Manns MP, Strassburg CP (2005) Identification and characterization of a functional TATA box polymorphism of the UDP glucuronosyltransferase 1A7 gene. Mol Pharmacol 67:1732–1739
17. Yamanaka H, Nakajima M, Katoh M, Hara Y, Tachibana O, Yamashita J, McLeod HL, Yokoi T (2004) A novel polymorphism in the promoter region of human UGT1A9 gene (UGT1A9*22) and its effects on the transcriptional activity. Pharmacogenetics 14:329–332
18. Carlini LE, Meropol NJ, Bever J, Andria ML, Hill T, Gold P, Rogatko A, Wang H, Blanchard RL (2005) UGT1A7 and UGT1A9 polymorphisms predict response and toxicity in colorectal cancer patients treated with capecitabine/irinotecan. Clin Cancer Res 11:1226–1236
19. Araki K, Fujita K, Ando Y, Nagashima F, Yamamoto W, Endo H, Miya T, Kodama K, Narabayashi Y, Sasaki Y (2006) Pharmacogenetic impact of polymorphisms in the coding region of the *UGT1A1* gene on SN-38 glucuronidation in Japanese patients with cancer. Cancer Sci 97:1255–1259
20. Saeki M, Saito Y, Jinno H, Sai K, Ozawa S, Kurose K, Kaniwa N, Komamura K, Kotake T, Morishita H, Kamakura S, Kitakaze M, Tomoike H, Shirao K, Tamura T, Yamamoto N, Kunitoh H, Hamaguchi T, Yoshida T, Kubota K, Ohtsu A, Muto M, Minami H, Saijo N, Kamatani N, Sawada JI (2006) Haplotype structures of the UGT1A gene complex in a Japanese population. Pharmacogenomics J 6:63–75
21. Ando M, Ando Y, Sekido Y, Ando M, Shimokata K, Hasegawa Y (2002) Genetic polymorphisms of the UDP-glucuronosyltransferase 1A7 gene and irinotecan toxicity in Japanese cancer patients. Jpn J Cancer Res 93:591–597
22. Sai K, Saeki M, Saito Y, Ozawa S, Katori N, Jinno H, Hasegawa R, Kaniwa N, Sawada J, Komamura K, Ueno K, Kamakura S, Kitakaze M, Kitamura Y, Kamatani N, Minami H, Ohtsu A, Shirao K, Yoshida T, Saijo N (2004) UGT1A1 haplotypes associated with reduced glucuronidation and increased serum bilirubin in irinotecan-administered Japanese patients with cancer. Clin Pharmacol Ther 75:501–515
23. Huang MJ, Yang SS, Lin MS, Huang CS (2005) Polymorphisms of uridine-diphosphoglucuronosyltransferase 1A7 gene in Taiwan Chinese. World J Gastroenterol 11:797–802
24. Girard H, Court MH, Bernard O, Fortier LC, Villeneuve L, Hao Q, Greenblatt DJ, von Moltke LL, Perussed L, Guillemette C (2004) Identification of common polymorphisms in the promoter of the UGT1A9 gene: evidence that UGT1A9 protein and activity levels are strongly genetically controlled in the liver. Pharmacogenetics 14:501–515
25. Innocenti F, Liu W, Chen P, Desai AA, Das S, Ratain MJ (2005) Haplotypes of variants in the UDP-glucuronosyltransferase1A9 and 1A1 genes. Pharmacogenet Genomics 15:295–301
26. Paoluzzi L, Singh AS, Price DK, Danesi R, Mathijssen RH, Verweij J, Figg WD, Sparreboom A (2004) Influence of genetic variants in UGT1A1 and UGT1A9 on the in vivo glucuronidation of SN-38. J Clin Pharmacol 44:854–860
27. Akaba K, Kimura T, Sasaki A, Tanabe S, Ikegami T, Hashimoto M, Umeda H, Yoshida H, Umetsu K, Chiba H, Yuasa I, Hayasaka K (1998) Neonatal hyperbilirubinemia and mutation of the bilirubin uridine diphosphate-glucuronosyltransferase gene: a common missense mutation among Japanese, Koreans and Chinese. Biochem Mol Biol Int 46:21–26
28. Bosma PJ, Chowdhury JR, Bakker C, Gantla S, de Boer A, Oostra BA, Lindhout D, Tytgat GN, Jansen PL, Oude Elferink RP (1995) The genetic basis of the reduced expression of bilirubin UDP-glucuronosyltransferase 1 in Gilbert's syndrome. N Engl J Med 333:1171–1175
29. Girard H, Villeneuve L, Court MH, Fortier LC, Caron P, Hao Q, von Moltke LL, Greenblatt DJ, Guillemette C (2006) The novel UGT1A9 intronic I399 polymorphism appears as a predictor of SN-38 glucuronidation levels in the liver. Drug Metab Dispos 34:1220–1228
30. Han JY, Lim HS, Shin ES, Yoo YK, Park YH, Lee JE, Jang IJ, Lee DH, Lee JS (2006) Comprehensive analysis of UGT1A polymorphisms predictive for pharmacokinetics and treatment outcome in patients with non-small-cell lung cancer treated with irinotecan and cisplatin. J Clin Oncol 24:2237–2244

Growth Stimulation of Non–Small Cell Lung Cancer Cell Lines by Antibody against Epidermal Growth Factor Receptor Promoting Formation of ErbB2/ErbB3 Heterodimers

Mari Maegawa,[1] Kenji Takeuchi,[1] Eishi Funakoshi,[1] Katsumi Kawasaki,[1] Kazuto Nishio,[2] Nobuyoshi Shimizu,[3] and Fumiaki Ito[1]

[1]Department of Biochemistry, Setsunan University; [2]Department of Genome Biology, Kinki University School of Medicine, Osaka, Japan; and [3]Department of Molecular Biology, Keio University School of Medicine, Tokyo, Japan

Abstract

Antibodies are the most rapidly expanding class of human therapeutics, including their use in cancer therapy. Monoclonal antibodies (mAb) against epidermal growth factor (EGF) receptor (EGFR) generated for cancer therapy block the binding of ligand to various EGFR-expressing human cancer cell lines and abolish ligand-dependent cell proliferation. In this study, we show that our mAb against EGFRs, designated as B4G7, exhibited a growth-stimulatory effect on various human cancer cell lines including PC-14, a non–small cell lung cancer cell line; although EGF exerted no growth-stimulatory activity toward these cell lines. Tyrosine phosphorylation of EGFRs occurred after treatment of PC-14 cells with B4G7 mAb, and it was completely inhibited by AG1478, a specific inhibitor of EGFR tyrosine kinase. However, this inhibitor did not affect the B4G7-stimulated cell growth, indicating that the growth stimulation by B4G7 mAb seems to be independent of the activation of EGFR tyrosine kinase. Immunoprecipitation with anti-ErbB3 antibody revealed that B4G7, but not EGF, stimulated heterodimerization between ErbB2 and ErbB3. ErbB3 was tyrosine phosphorylated in the presence of B4G7 but not in the presence of EGF. Further, the phosphorylation and B4G7-induced increase in cell growth were inhibited by AG825, a specific inhibitor of ErbB2. These results show that the ErbB2/ErbB3 dimer functions to promote cell growth in B4G7-treated cells. Changes in receptor-receptor interactions between ErbB family members after inhibition of one of its members are of potential importance in optimizing current EGFR family–directed therapies for cancer.

(Mol Cancer Res 2007;5(4):393–401)

Introduction

The epidermal growth factor (EGF) receptor (EGFR) is a member of the structurally related ErbB family of receptor tyrosine kinase. The ErbB family includes four members [i.e., EGFR (ErbB1), ErbB2, ErbB3, and ErbB4], all of which can dimerize with each other; in addition to homodimerization, specific ligands also induce heterodimerization of different pairs of the ErbB family members (1, 2). Although structural similarity exists between the family members, important differences are also present. Unlike the rest of the ErbB family, ErbB3 lacks tyrosine kinase activity (3, 4) and ErbB2 has no known ligand (5). EGF and transforming growth factor α bind directly only to EGFR, whereas neuregulins (also known as heregulins) are specific for ErbB3 and ErbB4 (6-8). Because expression levels of the family members and their ligands vary considerably in various cells, signaling pathways via activation of EGFR family members are complex.

Ligand-induced dimerization of EGFR is required to elevate its tyrosine kinase activity. The activated EGFR autophosphorylates tyrosine residues in its own COOH terminus, after which the receptor recruits and phosphorylates several signaling molecules such as growth factor receptor binding protein 2 (Grb-2), phospholipase Cγ, Src homology and collagen protein (Shc), and Grb2-associated binding protein 1 (Gab1; refs. 9, 10). Thus, ligands for EGFR are able to activate a variety of signaling pathways through their association with these signaling molecules. The mitogen-activated protein kinase (MAPK) pathway leading to phosphorylation of extracellular signal–regulated kinase (ERK)-1/2 plays an essential role in cell growth (9), and the phosphatidylinositol 3-kinase pathway is also important for cell growth and cell survival (11, 12). Another important signaling pathway is one for down-regulation of activated receptors. EGF binding is believed to result in localization of EGFR to clathrin-coated pits, from where EGFR is endocytosed. Recruitment of the Grb2/Casitas B-lineage lymphoma (Cbl) complex to the EGFR and subsequent activation of Cbl dependent ubiquitination are essential for the delivery of EGFRs into these clathrin-coated pits (13).

Received 9/18/06; revised 1/16/07; accepted 2/6/07.
Grant support: Grant-in-Aid for Scientific Research from Japan Society for the Promotion of Science; fund for "Research for the Future" Program from the Japan Society for the Promotion of Science and Ministry of Education, Culture, Sports, Science, and Technology; and funding from the Fugaku Trust for Medical Research.
The costs of publication of this article were defrayed in part by the payment of page charges. This article must therefore be hereby marked *advertisement* in accordance with 18 U.S.C. Section 1734 solely to indicate this fact.
Note: M. Maegawa and K. Takeuchi contributed equally to this work.
Requests for reprints: Fumiaki Ito, Department of Biochemistry, Faculty of Pharmaceutical Sciences, Setsunan University, 45-1 Nagaotoge-cho, Hirakata, Osaka 573-0101, Japan. Phone: 81-72-866-3115; Fax: 81-72-866-3117. E-mail: fito@pharm.setsunan.ac.jp

doi:10.1158/1541-7786.MCR-06-0303

Alterations resulting in enhanced EGFR expression or function have been documented in a variety of tumors, including non-small cell lung cancer, breast cancer, and gliomas (14-17). These changes can occur due to increased production of ligands such as EGF and transforming growth factor α, increased gene transcription or amplification of EGFR, and receptor mutations resulting in constitutive activation of the receptor tyrosine kinase (18, 19). A variety of approaches to block the EGFR mediated signaling pathway are currently undergoing clinical evaluation, including the use of anti-EGFR monoclonal antibodies (mAb), low molecular weight tyrosine kinase inhibitors, and immunoconjugates (20, 21). A series of anti-EGFR mAbs produced showed inhibitory activity toward the binding of EGF to A431 cells (22). As a result of the inhibition of receptor kinase, these anti-EGFR mAbs prevented ligand-induced stimulation of growth in a variety of cells that expressed both EGFR and ligand (20). It was also reported that anti-EGFR mAbs have the capacity to form receptor-containing complexes that result in receptor internalization, an important mechanism for attenuating receptor signaling (23).

It is important to further explore the primary mechanism by which various antibodies against EGFR affect growth of a variety of cells. In this present study, we decided to examine the growth-inhibitory effect of a mouse anti-human EGFR mAb, B4G7, which had previously been prepared against human A431 cells (24). Contrary to our expectations, B4G7 actually exhibited a growth-stimulatory effect in a variety of cells including gefitinib-sensitive and gefitinib-resistant non-small cell lung cancer cell lines, PC-9 and PC-14, respectively. Because EGF showed no stimulatory effect on the growth of these cell lines, we studied the molecular effects of B4G7 mAb and EGF in more detail. Our results indicate that mAb against EGFR increased growth of several cancer cell lines by stimulating the formation of ErbB2/ErbB3 heterodimers. Therefore, it is of importance to consider the status of all ErbB family members in cancer cells, not just the EGFR, for optimizing EGFR-directed cancer therapies.

Results

Growth-Stimulatory Activity of mAb against EGFR

We previously produced a mouse anti-human EGFR mAb against A431 cells and referred to it as B4G7 (24). In this study, we first examined the effect of the B4G7 mAb on the growth of various human cancer cell lines. The mAb exhibited a growth-stimulatory effect on human non-small cell lung cancer cell lines (PC-9, PC-14, and A549) as well as on A431 human epidermoid carcinoma cells, as determined from the results of a colorimetric assay (Fig. 1). The growth-stimulatory action of B4G7 was confirmed by counting the number of PC-14 cells in the presence or absence of B4G7 (data not shown). We also examined the mitogenic activity of purified mouse immunoglobulin G (IgG) toward PC-14 cells and found that their growth was not affected by this control IgG (data not shown). These were unexpected results because many research groups have previously reported that anti-EGFR mAbs block the binding of ligand to various EGFR-expressing human cancer cell lines and thereby abolish ligand-dependent cell proliferation (20). Because EGF showed no stimulatory effect on the growth of these cell lines, we next studied the molecular effects of B4G7 mAb and EGF on EGFR.

B4G7 mAb Affects Neither the Internalization nor the Down-Regulation of EGFR in PC-14 Cells

As shown in Fig. 2A, the majority of EGFRs were localized at the cell surface in the control cells. After EGF stimulation, the distribution of EGFRs was quite distinct: the cell-surface receptors disappeared; and EGFR-containing vesicles appeared in their place, thus indicating the internalization of EGFR on

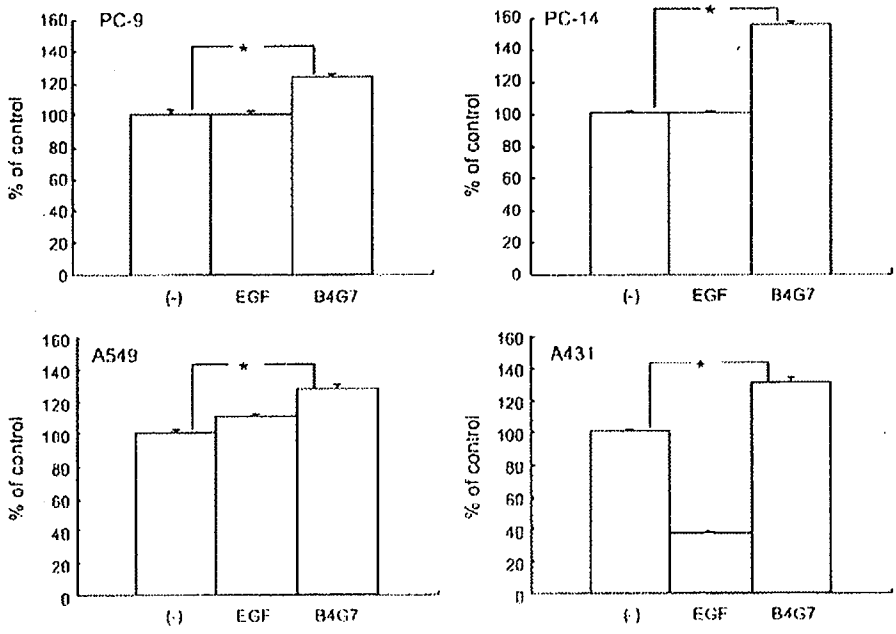

FIGURE 1. Growth-stimulatory effect of anti-EGFR mAb. Cells were treated or not with 100 ng/mL EGF or 10 μg/mL B4G7 for 2 d and their growth was estimated by means of WST-1 assay as described in Materials and Methods. Columns, mean ($n = 6$); bars, SD. *, $P < 0.01$. Similar results were obtained from five independent experiments.

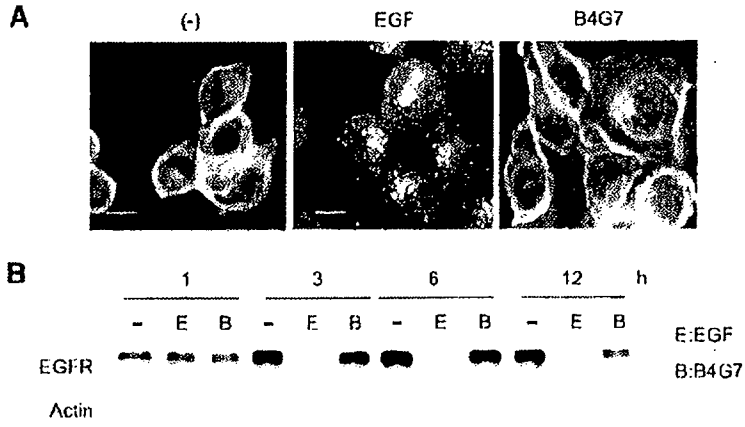

FIGURE 2. B4G7 affects neither the internalization nor the down-regulation of EGFR in PC-14 cells. **A.** PC-14 cells were treated with 100 ng/mL EGF or 10 μg/mL B4G7 mAb for 15 min. EGFR localization of these cells was determined by immunostaining as described in Materials and Methods. Bar, 10 μm. **B.** PC-14 cells were treated or not with EGF or B4G7 for the indicated times. Cell lysates were prepared and used for the detection of EGFR as described in Materials and Methods. The blot was reprobed with a β-actin antibody to show equal loading. Similar results were obtained from four independent experiments. Immunoblot analyses of total cellular lysates, which were prepared by using the Laemmli SDS buffer containing 5% mercaptoethanol, gave similar results.

EGF stimulation. In contrast, most of EGFRs still remained on the cell surface after B4G7 treatment. We next did Western blot analysis to assess the down-regulation of EGFRs after stimulation of PC-14 cells with EGF or B4G7 mAb (Fig. 2B). The down-regulation increased as the incubation time with EGF was lengthened, whereas EGFRs were still detected even 12 h after B4G7 treatment. Thus, B4G7 mAb affected neither the internalization nor the down-regulation of EGFRs.

Activation of EGFR, ERK1/2, and Akt after B4G7 Treatment

Next, we assessed EGFR phosphorylation on Tyr^{1173} and phosphorylation of ERK1/2 and Akt, downstream molecules of EGFR, after stimulation of PC-14 cells with EGF or B4G7 mAb (Fig. 3). Following the addition of EGF or B4G7, tyrosine phosphorylation of EGFR was observed with a peak at 10 to 15 min. ERK1/2 and Akt were phosphorylated even in the absence of EGF or B4G7, and this phosphorylation was further augmented in both EGF- and B4G7-treated cells. It thus seems that the growth-stimulatory activity of B4G7 mAb is not simply explained by its activity to stimulate tyrosine phosphorylation of EGFR and subsequent phosphorylation of ERK1/2 and Akt molecules. Figure 3 also shows the effect of AG1478, a specific inhibitor of EGFR tyrosine kinase, on tyrosine phosphorylation of EGFR. This inhibitor suppressed the tyrosine phosphorylation of EGFR in both EGF- and B4G7-treated cells, although a

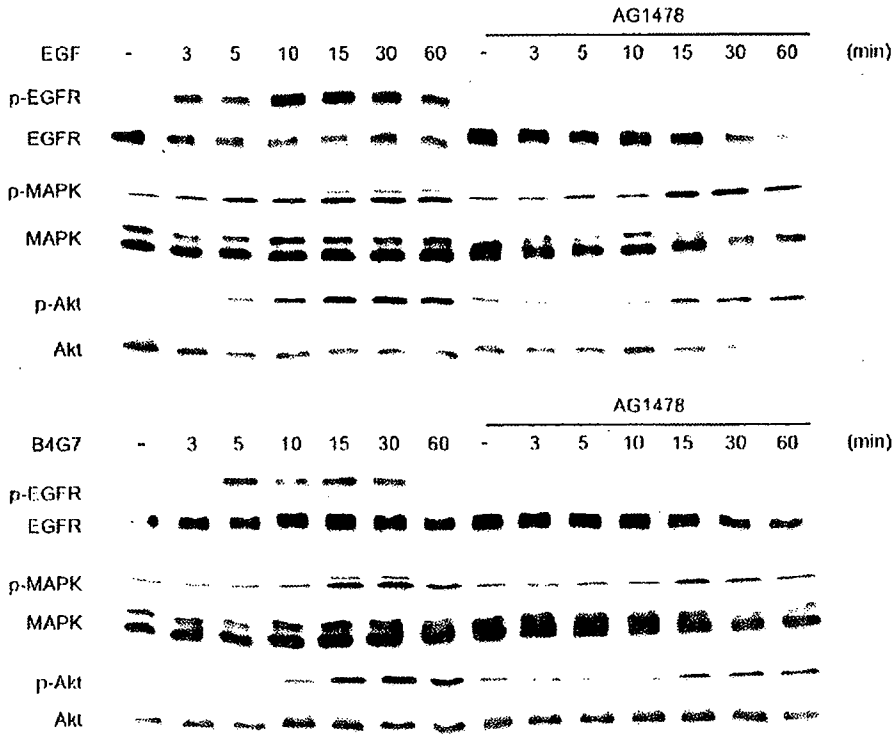

FIGURE 3. AG1478 inhibits tyrosine phosphorylation of EGFR but not phosphorylation of Akt and ERK1/2. PC-14 cells were pretreated with 200 nmol/L AG1478 for 2 h and then incubated with EGF or B4G7 for the indicated times. Total cell extracts were then prepared and electrophoresed on 7.5% SDS-PAGE for the detection of EGFR phosphorylation or on 12.5% SDS-PAGE for the detection of phosphorylated ERK1/2 and phosphorylated Akt. EGFR, ERK1/2, and Akt and phosphorylation of these molecules were detected by using each corresponding antibody. Similar results were obtained from three independent experiments.

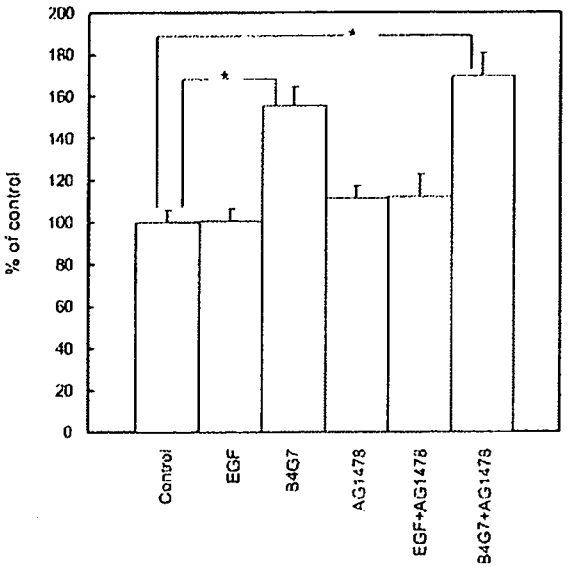

FIGURE 4. AG1478 shows no inhibitory activity against B4G7-stimulated cell growth. PC-14 cells were pretreated with 200 nmol/L AG1478 for 2 h and then incubated with 100 ng/mL EGF or 10 μg/mL B4G7. After 2 d of incubation, their growth was estimated by means of the WST-1 assay as described in Materials and Methods. Columns, mean ($n = 6$); bars, SD. *, $P < 0.01$. Similar results were obtained from three independent experiments.

faint band of phosphorylated EGFR band was still visible in EGF-treated cells after AG1478 treatment. On the other hand, the inhibitory activity of the inhibitor against the phosphorylation of ERK1/2 and Akt was not remarkable. This result suggests that activation of the two signaling proteins ERK1/2 and Akt in B4G7-treated cells occurred via a pathway independent of the tyrosine phosphorylation of EGFR.

Next, we determined the effect of AG1478 on the B4G7-stimulated cell growth (Fig. 4). This inhibitor showed no inhibitory activity against the stimulation of PC-14 cell growth, indicating that the growth stimulation by B4G7 mAb seems to have been independent of the activation of EGFR tyrosine kinase.

Stimulated Formation of HER2/HER3 Heterodimer by B4G7

EGFR, ErbB2, ErbB3, and ErbB4 are members of the ErbB family of receptors. ErbB receptors signal through a network involving receptor homodimerization and heterodimerization. Thus, we examined whether B4G7 mAb would cause the down-regulation of other members of the ErbB family although it did not down-regulate EGFR. As shown in Fig. 5A, incubation of PC-14 cells with EGF, but not with B4G7 mAb, caused down-regulation of ErbB2. On the other hand, neither EGF nor B4G7 mAb down-regulated ErbB3. Many studies have shown that ligand-activated EGFRs preferentially recruit ErbB2 into a heterodimeric complex in cells that coexpress ErbB2 (25). Thus, it is most likely that EGF down-regulated ErbB2 through the increased formation of EGFR/ErbB2 heterodimer. In fact, when lysates from EGF-treated PC-14 cells were incubated with anti-EGFR antibody, ErbB2 became detectable in the immunocomplex (Fig. 5B). In contrast, it was not detected in lysates from B4G7-treated PC-14 cells.

ErbB3 has been observed to preferentially heterodimerize with ErbB2 in several cancers, leading to a strong oncogenic signal thought to promote tumor cell proliferation (26). We thus studied whether treatment of PC-14 cells with EGF or B4G7 would affect complex formation between ErbB2 and ErbB3. Immunoprecipitation with anti-ErbB3 antibody revealed that

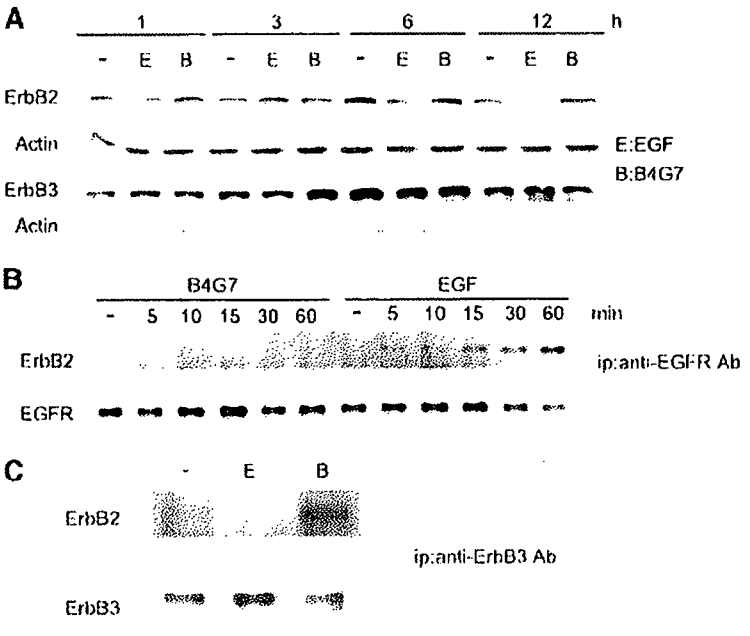

FIGURE 5. B4G7 stimulates ErbB2/ErbB3 heterodimer formation. **A.** PC-14 cells were treated or not with EGF or B4G7 for the indicated times. Lysates were prepared from these cells and used for the detection of ErbB2 and ErbB3 as described in Materials and Methods. The blot was reprobed with a β-actin antibody to show equal loading. **B.** EGFR was immunoprecipitated from the lysates by using anti-EGFR antibody, and the immunoprecipitates were examined for EGFR and ErbB2 as described in Materials and Methods. **C.** PC-14 cells were treated or not with EGF or B4G7 for 15 min. The supernatant fractions of cell lysates were immunoprecipitated with anti-c-erbB3 antibody, and proteins eluted from the immunocomplexes were subjected to SDS-PAGE and used for immunoblot analysis of ErbB2 and ErbB3. Similar results were obtained from three independent experiments.

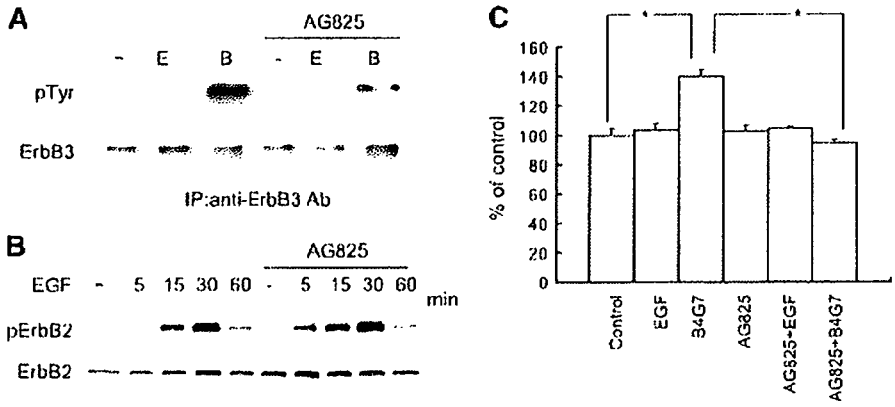

FIGURE 6. AG825 inhibits tyrosine phosphorylation of ErbB3 and cell growth in B4G7-treated cells. **A.** PC-14 cells were pretreated with 0.5 μmol/L AG825 for 2 h and then treated with EGF or B4G7 for 15 min. The cells were then subjected to immunoprecipitation with anti-c-erbB3 antibody and used for the detection of ErbB3 and its tyrosine phosphorylated form by using anti-ErbB3 antibody and anti-phosphotyrosine antibody (PY20). **B.** PC-14 cells were incubated with EGF for the indicated times after AG825 (0.5 μmol/L) pretreatment. Cell lysates were then prepared and used for immunoblot analysis of ErbB2 and its phosphorylation by using anti-c-ErbB2 antibody and anti-phospho-erbB2 (Tyr^{1248}) antibody, respectively. **C.** PC-14 cells were incubated with EGF or B4G7 for 2 d in the presence of 0.5 μmol/L AG825. Their growth was estimated by means of the WST-1 assay as described in Materials and Methods. Columns, mean ($n = 6$); bars, SD. *, $P < 0.01$. Similar results were obtained from three independent experiments.

B4G7 but not EGF stimulated heterodimerization between ErbB2 and ErbB3 (Fig. 5C).

The EGFR extracellular domain (amino acids 1-621) shares 45% amino acid identity with that of ErbB3. Due to this homology, specific B4G7 antibody against EGFR may show some cross-reactivity against ErbB3. We thus determined whether B4G7 binds to ErbB3 as well as to EGFR. Immunocomplexes were prepared from lysates of PC-14 cells using B4G7 and assayed for the presence of ErbB3 by immunoblot analysis. Because ErbB3 was not detected at all in these complexes (data not shown), B4G7 seems to promote formation of ErbB2/ErbB3 heterodimers by its binding to EGFR but not to ErbB3.

B4G7-Stimulated Cell Growth Requires ErbB2/ErbB3 Heterodimer and ErbB3 Tyrosine Phosphorylation

If ErbB2/ErbB3 heterodimers are formed in the presence of B4G7, ErbB3 of B4G7-treated cells could be phosphorylated by ErbB2 tyrosine kinase. Indeed, ErbB3 was tyrosine phosphorylated in the presence of B4G7 but not in the presence of EGF (Fig. 6A). Further, this phosphorylation was inhibited by AG825, a specific inhibitor of ErbB2. On the contrary, EGF-induced phosphorylation of ErbB2 at Tyr^{1248}, possibly through heterodimerization of EGFR/ErbB2, was not inhibited by AG825 (Fig. 6B), indicating a selective inhibitory action of this inhibitor against ErbB2 tyrosine kinase. Further analysis of immunocomplexes formed in the presence of anti-EGFR antibody confirmed that ErbB2 phosphorylation by EGFR tyrosine kinase was not inhibited by this inhibitor; tyrosine-phosphorylated ErbB2 was detected only in the immunocomplexes from EGF-treated cells but not in those from B4G7 treated cells, and this phosphorylation was not inhibited by AG825 (data not shown).

To examine association of ErbB2 tyrosine kinase with B4G7-induced cell growth, we treated PC-14 cells with AG825 before their stimulation with EGF or B4G7. As shown in Fig. 6C, cell growth increased by B4G7 was suppressed to the control level by this pretreatment. These results show that ErbB2 tyrosine kinase and the ErbB2/ErbB3 dimer function to promote cell growth in B4G7-treated cells.

Discussion

We previously produced a mAb against EGFRs by immunizing BALB/c mice with human epidermoid carcinoma A431 cells (24). This mAb, which we named B4G7, inhibited the binding of ^{125}I-EGF to A431 cells and human fibroblasts and specifically precipitated EGFR of A431 cells. Sato et al. (22) also produced mAbs against A431 cells and found that these antibodies were capable of inhibiting both the binding of EGF to its receptor and ligand-induced cell proliferation. In this study, we made the unexpected finding that B4G7 mAb exerted growth-stimulatory activity toward various cancer cell lines. We initially thought that B4G7 stimulated cell growth via signaling pathways originating from EGFR tyrosine phosphorylation because B4G7 stimulated EGFR tyrosine phosphorylation and also phosphorylation of MAPK and Akt, two downstream signaling molecules of EGFR. However, the growth stimulation by B4G7 was independent of EGFR activation itself because the stimulation was not affected by the presence of AG1478, an EGFR tyrosine kinase-specific inhibitor.

EGFR forms homodimers as well as heterodimers with the other ErbB family members, and cooperation between ErbB family members plays pivotal roles in a variety of critical functions. It is thus reasonable to speculate that binding of B4G7 mAb to EGFR affects cross-talk among the ErbB family and the cellular effects mediated by these receptors. In B4G7-treated PC-14 cells, the EGFR/ErbB2 complex was not detected, although its formation was increased in response to EGF (Fig. 5B). Therefore, B4G7 may have blocked the ability of EGFR to heterodimerize with ErbB2 or ErbB3 and thus facilitated enhanced dimerization between ErbB2 and ErbB3. In fact, ErbB2/ErbB3 heterodimers were formed in the presence of

B4G7 but not in the presence of EGF (Fig. 5C). In EGF-treated PC-14 cells, major combinations of ErbB family members were EGFR homodimer and EGFR/ErbB2 heterodimer. AG1478 inhibited, but not completely, EGFR phosphorylation, whereas it inhibited phosphorylation of ERK1/2 and Akt to a lesser extent. The limited efficacy of AG1478 could have arisen from unblocked ErbB2 signaling in the form of EGFR/ErbB2.

At least six different ligands are known to bind to EGFR. These ligands include EGF, transforming growth factor α, amphiregulin, heparin-binding EGF, betacellulin, and epiregulin (1, 20, 27). A second class of ligands, collectively termed neuregulin, bind directly to ErbB3 and/or ErbB4 (6-8). It is known that ErbB2 and ErbB3 dimerize to produce a high-affinity receptor for neuregulin-1. Because production and secretion of neuregulin-1 have been reported in many human lung cancer cell lines (28), it is very likely that neuregulin-1 or neuregulin isoform is secreted from PC-14 cells and thereafter activates the ErbB2/ErbB3 heterodimer in an autocrine fashion. This likelihood is supported by the finding that ErbB3 phosphorylation was increased on B4G7 addition and abrogated in the presence of AG825, which selectively inhibits the ErbB2 kinase activity.

The physiologic role of ErbB2, in the context of ErbB ligand signaling, is to serve as a coreceptor (29, 30). ErbB2 seems to be the preferred partner of the other ligand-bound ErbBs (25, 31). ErbB3 functions as an indispensable ErbB2 dimerization partner and is required for proliferation of ErbB2-overexpressing tumor cells, and neither ErbB1 nor ErbB4 could replace ErbB3 as partner of ErbB2 to drive proliferation. Therefore, it seems that the ErbB2/ErbB3 formed in the presence of B4G7 but not in the presence of EGF transmits effective proliferation signals in PC-14 cells. This notion is supported by our finding that AG825, a specific inhibitor of ErbB2, suppressed B4G7-stimulated cell growth (Fig. 6C). Taken together, these findings indicate that B4G7 transmitted signals for growth stimulation by increasing the formation of ErbB2/ErbB3 (see Fig. 7).

The signals generated by activated growth factor receptors are generally attenuated by the process of receptor internalization, which leads to receptor degradation (32, 33). Neuregulin has been reported to undergo slow endocytosis followed by receptor recycling to the plasma membrane (34). In contrast, most of the EGF-stimulated EGFR molecules are destined to lysosomal degradation. Due to the consequent clearance of EGFR but not ErbB3 molecules from the cell surface, the mitogenic signal evoked by EGF is less potent than the neuregulin signal (29). In PC-14 cells, EGFR and ErbB2 were down-regulated in the presence of EGF, but their levels were unchanged after B4G7 treatment. Therefore, slow endocytosis and receptor recycling of ErbB2 and ErbB3 may explain the capacity of B4G7 to deliver more sustained mitogenic signals than EGF. Another mechanism for the different mitogenic capacity probably involves the recruitment of distinct sets of downstream effectors to each of the activated ErbB family members. One of the downstream effectors is phosphatidylinositol 3-kinase, the activation of which results in the phosphorylation of the 3′ position of phosphatidylinositol 4,5-bis-phosphate to yield phosphatidylinositol 3,4,5-tris-phosphate. Phosphatidylinositol 3,4,5-tris-phosphate, in turn, activates several downstream signaling molecules including Akt. ErbB3 effectively couples to the phosphatidylinositol 3-kinase/Akt pathway because it has six tyrosine phosphorylation sites with YXXMs motifs, which serve as excellent binding sites for phosphatidylinositol 3-kinase (35, 36). Because the phosphatidylinositol 3-kinase/Akt pathway originating from ErbB3 is suggested to play an important role in the stimulation of cell growth (37, 38), it is reasonable to speculate that this pathway is linked to the mitogenic superiority of ErbB3. In this study, we determined the phosphorylation time course of Akt in B4G7- and EGF-treated cells, but there was no significant difference between their phosphorylation kinetics.

Neuregulin activates ERK MAPK, a signaling pathway that is critical in the mitogenic effect of neuregulin (39, 40). It has been indicated that sustained, but not transient, activation of ERK induces phosphorylation of immediate early gene products, which leads to their stabilization and activation, resulting in appropriate gene expression, such as that of cyclin D (41, 42). Further, only sustained ERK activation induces and maintains decreased expression levels of antiproliferative genes (43). Thus, the duration and magnitude of ERK activity is a key determinant for the mitogenic response of various cells to EGF (44, 45). The differential mitogenic response of PC-14 cells to

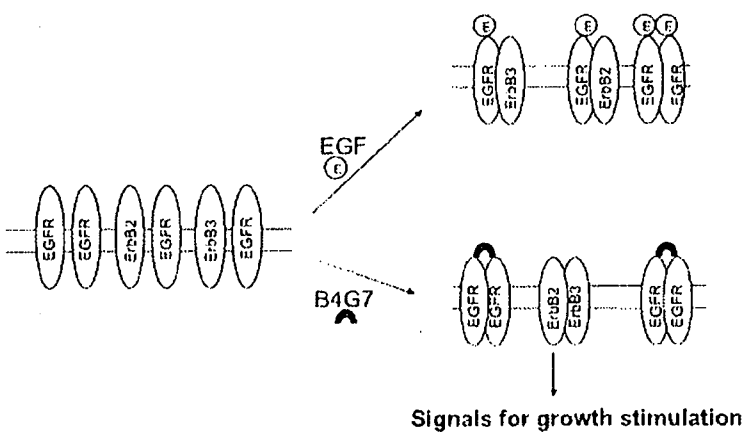

FIGURE 7. Schematic representation of how mAb B4G7 stimulates cell growth. Homodimers and heterodimers of EGFR are formed on EGF addition. On the other hand, the ErbB2/ErbB3 heterodimer is formed in the presence of B4G7 mAb because binding of B4G7 mAb to EGFR inhibits the ability of EGFR to form heterodimers with ErbB2 and ErbB3. ErbB2/ErbB3, unlike EGFR dimers, continues to exist on the cell surface and transmits signals for growth stimulation. ErbB2/ErbB3 may be activated in an autocrine fashion.

EGF and B4G7 may be related to the differential kinetics of ERK activation in B4G7- and EGF-treated cells. However, both EGF and B4G7 mAb stimulated phosphorylation of ERK in a similar time-dependent manner (see Fig. 3). We studied phosphorylation of ERK and Akt in PC-14 cells treated with EGF or B4G7 for a longer period of time, but observed no significant difference in the phosphorylation time course between B4G7- and EGF-treated cells.[4] The duration of Akt and MAPK activities may be essential, but not sufficient, for ensuring G_1 phase progression of PC-14 cells. A more detailed side-by-side comparison of PC-14 cells treated with EGF or B4G7 should provide a hint for elucidating the signaling pathway for B4G7-induced cell growth.

A variety of approaches to block the EGFR-mediated signaling pathway are undergoing clinical evaluation, including the use of mAbs against EGFR and ErbB2 (46). The study presented here might have important clinical implications because it indicates that mAb against EGFR stimulated the growth of several cancer cell lines by affecting dimerization of EGFR family members other than EGFR. Similarly, ZD1839, a specific EGFR tyrosine kinase inhibitor, has been reported to inhibit the growth of ErbB2-overexpressing breast cancer cells, possibly by sequestration of ErbB2 and ErbB3 receptors in an inactive heterodimer configuration with EGFR (47). Another group also reported that elimination of ErbB2 signaling resulted in an increase in EGFR expression and activation and that its increased activation contributed to sustained cell survival (48). Changes in receptor-receptor interactions between ErbB family members and compensatory changes in the ErbB family after inhibition of one of its members are of potential importance in optimizing current EGFR family directed therapies for cancer.

Materials and Methods

Materials

EGF (ultrapure) from mouse submaxillary glands was purchased from Toyobo Co. Ltd. (Osaka, Japan). FCS, phenylmethylsulfonyl fluoride, pepstatin A, *p*-toluenesulfonyl-L-arginine methyl ester, leupeptin, and aprotinin came from Sigma (St. Louis, MO). AG1478 [4-(3-chloroanilino)-6,7-dimethoxyquinazoline] and AG825 [4-hydroxy-3-methoxy-5-(benzothiazolylthiomethyl)benzylidenecyanoacetamide] were purchased from Calbiochem (San Diego, CA). RPMI 1640 and DMEM were from Nissui Pharmaceutical Co. Ltd. (Tokyo, Japan). Antibodies used and their sources were as follows: anti-phosphotyrosine (PY20; BD Transduction Laboratories, San Jose, CA); anti-phospho-EGFR (Tyr^{1173}) and anti phospho-erbB2 (Tyr^{1248}) (Upstate Biotechnology, Lake Placid, NY); anti-EGFR (1005) and anti-ErbB3 (C-17; Santa Cruz Biotechnology, Inc., Santa Cruz, CA); anti-Akt (Cell Signaling Technology, Inc., Beverly, MA); anti-MAPK (Sigma); anti phospho-Akt (Tyr^{473}) and anti-ACTIVE MAPK (Promega, Madison, WI); anti c-ErbB2/c-Neu (Ab-3; Calbiochem); horseradish peroxidase conjugated swine anti-rabbit immunoglobulin (DAKO, Glostrup, Denmark); and horseradish peroxidase linked sheep anti-mouse IgG and biotinylated sheep anti-mouse immunoglobulin (GE Healthcare, Piscataway, NJ). A mouse anti-human EGFR mAb (B4G7) was purified from mouse ascites by ammonium sulfate precipitation and protein G column chromatography. All other chemicals were commercial products of reagent grade.

Cell Culture

Human non-small cell lung cancer cell lines PC-9 and PC-14 were obtained from Tokyo Medical University (Tokyo, Japan). Both lines were cultured in RPMI 1640 supplemented with 5% FCS in 5% CO_2 at 37°C in a fully humidified atmosphere. Human adenocarcinoma A549 and epidermoid carcinoma A431 were cultured in DMEM supplemented with 5% FCS. Exponentially growing cells were used in all experiments.

Growth Stimulation Assay

Cells were seeded at a density of 2×10^3 per well into a 96-well microtiter plate and cultured for 2 days in the presence of 5% FCS. They were then treated with 100 ng/mL EGF or 10 μg/mL B4G7 mAb. After incubation for 48 h, growth stimulation was quantified by a colorimetric assay with the WST-1 reagent according to the manufacturer's instruction (Dojindo Laboratories, Kumamoto, Japan).

Preparation of Cellular Lysates and Immunoblotting

PC-14 cells were seeded at a density of 1.2×10^5 per 35-mm-diameter dish and cultured for 2 days. They were then treated or not with 100 ng/mL EGF or 10 μg/mL B4G7 mAb for indicated times at 37°C. When the effects of AG1478 or AG825 were assayed, these inhibitors were added 2 h before the addition of EGF or B4G7. The cells were then washed with ice-cold PBS and subsequently lysed by incubating in hypotonic buffer [10 mmol/L Tris-HCl (pH 7.8), containing 10 mmol/L NaCl, 1.5 mmol/L $MgCl_2$, 0.5 mmol/L DTT, 0.5 mmol/L phenylmethylsulfonyl fluoride, 2 μg/mL leupeptin, 2 μg/mL aprotinin, and 0.3% NP40]. The lysates were incubated on ice for 10 min and clarified by centrifugation at $1,500 \times g$ for 5 min at 4°C. Total proteins (10 μg/mL) from the supernatant fractions were resolved by SDS-PAGE and transferred to Immobilon-P membrane (Millipore, Bedford, MA). The membranes were sequentially incubated, first with primary antibody for 2 h and then with horseradish peroxidase-conjugated anti-rabbit IgG antibody (1:1,000) or anti-mouse IgG antibody (1:1,000) for 1 h. Finally, the proteins were visualized by use of an enhanced chemiluminescence Western Blotting Detection System (GE Healthcare) and exposed to autoradiography film (Fuji Medical X-ray film RX-U, Fuji Photo Film Co., Ltd., Tokyo, Japan).

Immunostaining of Cells for Confocal Laser Scanning Microscopic Observation

Immunostaining of cells was done as previously described (49). Briefly, PC-14 cells were grown on coverslips for 2 days and then stimulated with 100 ng/mL EGF or 10 μg/mL B4G7 mAb for 15 min. The cells were fixed with methanol for 5 min at −20°C, after which they were washed thrice with 20 mmol/L TBS (pH 7.4) containing 1 mmol/L $CaCl_2$ (TBS-Ca) and incubated with anti-EGFR antibody for 2 h at room temperature.

[4] Kenji Takeuchi and Fumiaki Ito, unpublished data.

After being washed with TBS-Ca, the cells were incubated with biotinylated sheep anti-mouse immunoglobulin antibody (1:100) for 1 h at room temperature and then with Texas red labeled streptavidin (GE Healthcare). The stained cells were observed under a confocal laser scanning microscope (MRC1024, Bio-Rad, Hercules, CA).

Immunoprecipitation

PC-14 cells were seeded at 1.2×10^6 per 150-mm dish and incubated in RPMI 1640/5% FCS for 2 days. The cultures were then incubated for 2 h in the presence or absence of 0.5 μmol/L AG825 and treated with either EGF or B4G7 for the indicated times at 37°C. They were lysed in hypotonic buffer and centrifuged at 1,500 × *g* for 5 min as described above. The supernatant fractions were incubated overnight at 4°C with anti-c-erbB3 (clone 2F12) antibody (LabVision Co., Fremont, CA) or anti-EGFR antibody (B4G7). Immunocomplexes were collected on protein G-sepharose (GE Healthcare). Bound proteins were washed thrice with 10 mmol/L Tris-HCl buffer (pH 7.4) containing 135 mmol/L NaCl, 0.1% NP40, 0.1% Triton X-100, a cocktail of protease inhibitors (0.1 mg/mL phenylmethylsulfonyl fluoride, 2 μg/mL leupeptin, 1 μg/mL pepstatin A, 0.1 μg/mL *p*-toluenesulfonyl-L-arginine methyl ester), 1 mmol/L sodium orthovanadate, 2 mmol/L EGTA, 5 mmol/L EDTA, 50 mmol/L sodium fluoride, and 30 mmol/L $Na_4P_2O_7$ and once with TBS and eluted in Laemmli sample buffer containing 2-mercaptoethanol. Eluted proteins were subjected to SDS-PAGE and immunoblotted as described above.

Protein Assay

Protein content was assayed by using a Coomassie Plus Protein Assay reagent (Pierce Chemical Co., Rockford, IL) according to the manufacturer's instructions.

References

1. Olayioye MA, Neve RM, Lane HA, Hynes NE. The ErbB signaling network: receptor heterodimerization in development and cancer. EMBO J 2000;19:3159–67.

2. Yarden Y, Sliwkowski MX. Untangling the ErbB signalling network. Nat Rev Mol Cell Biol 2001;2:127–37.

3. Sliwkowski MX, Schaefer G, Akita RW, et al. Coexpression of erbB2 and erbB3 proteins reconstitutes a high affinity receptor for heregulin. J Biol Chem 1994;269:14661–5.

4. Guy PM, Platko JV, Cantley LC, Cerione RA, Carraway KL III. Insect cell-expressed p180erbB3 possesses an impaired tyrosine kinase activity. Proc Natl Acad Sci U S A 1994;91:8132–6.

5. Klapper LN, Glathe S, Vaisman N, et al. The ErbB-2/HER2 oncoprotein of human carcinomas may function solely as a shared coreceptor for multiple stroma-derived growth factors. Proc Natl Acad Sci U S A 1999;96:4995–5000.

6. Tzahar E, Levkowitz G, Karunagaran D, et al. ErbB-3 and ErbB-4 function as the respective low and high affinity receptors of all Neu differentiation factor/heregulin isoforms. J Biol Chem 1994;269:25226–33.

7. Lupu R, Colomer R, Kannan B, Lippman ME. Characterization of a growth factor that binds exclusively to the erbB-2 receptor and induces cellular responses. Proc Natl Acad Sci U S A 1992;89:2287–91.

8. Holmes WE, Sliwkowski MX, Akita RW, et al. Identification of heregulin, a specific activator of p185erbB2. Science 1992;256:1205–10.

9. Schlessinger J. Cell signaling by receptor tyrosine kinases. Cell 2000;103:211–25.

10. Ruff-Jamison S, McGlade J, Pawson T, Chen K, Cohen S. Epidermal growth factor stimulates the tyrosine phosphorylation of SHC in the mouse. J Biol Chem 1993;268:7610–2.

11. Marte BM, Downward J. PKB/Akt: connecting phosphoinositide 3-kinase to cell survival and beyond. Trends Biochem Sci 1997;22:355–8.

12. Takeuchi K, Ito F. Suppression of Adriamycin-induced apoptosis by sustained activation of the phosphatidylinositol-3′-OH kinase-Akt pathway. J Biol Chem 2004;279:892–900.

13. Stang E, Blystad FD, Kazazic M, et al. Cbl-dependent ubiquitination is required for progression of EGF receptors into clathrin-coated pits. Mol Biol Cell 2004;15:3591–604.

14. Lynch TJ, Bell DW, Sordella R, et al. Activating mutations in the epidermal growth factor receptor underlying responsiveness of non-small-cell lung cancer to gefitinib. N Engl J Med 2004;350:2129–39.

15. Arteaga CL. Epidermal growth factor receptor dependence in human tumors: more than just expression? Oncologist 2002;7(Suppl 4):31–9.

16. Humphrey PA, Gangaiosa LM, Weng AJ, et al. Deletion-mutant epidermal growth factor receptor in human gliomas: effects of type II mutation on receptor function. Biochem Biophys Res Commun 1991;178:1413–20.

17. Wong AJ, Bigner SH, Bigner DD, Kinzler KW, Hamilton SR, Vogelstein B. Increased expression of the epidermal growth factor receptor gene in malignant gliomas is invariably associated with gene amplification. Proc Natl Acad Sci U S A 1987;84:6899–903.

18. Janssen RN, Walker F, Pouliot N, Garrett TP, Ward CW, Burgess AW. Epidermal growth factor receptor: mechanisms of activation and signalling. Exp Cell Res 2003;284:31–53.

19. Chu CT, Everiss KD, Wikstrand CJ, Batra SK, Kung HJ, Bigner DD. Receptor dimerization is not a factor in the signalling activity of a transforming variant epidermal growth factor receptor (EGFRvIII). Biochem J 1997;324:855–61.

20. Mendelsohn J, Baselga J. The EGF receptor family as targets for cancer therapy. Oncogene 2000;19:6550–65.

21. Herbst RS, Onn A, Mendelsohn J. The role of growth factor signaling in malignancy. In: Frank DA, editor. Signal transduction in cancer. Boston/Dordrecht/London: Kluwer Academic Publishers; 2003. p. 19–72.

22. Sato JD, Kawamoto T, Le AD, Mendelsohn J, Polikoff J, Sato GH. Biological effects *in vitro* of monoclonal antibodies to human epidermal growth factor receptors. Mol Biol Med 1983;1:511–29.

23. Fan Z, Lu Y, Wu X, Mendelsohn J. Antibody-induced epidermal growth factor receptor dimerization mediates inhibition of autocrine proliferation of A431 squamous carcinoma cells. J Biol Chem 1994;269:27595–602.

24. Behrzadian MA, Shimizu N. Monoclonal antibody that immunoreacts with a subclass of human receptors for epidermal growth factor. Cell Struct Funct 1985;10:219–32.

25. Graus-Porta D, Beerli RR, Daly JM, Hynes NE. ErbB-2, the preferred heterodimerization partner of all ErbB receptors, is a mediator of lateral signaling. EMBO J 1997;16:1647–55.

26. Holbro T, Beerli RR, Maurer F, Koziczak M, Barbas CF III, Hynes NE. The ErbB2/ErbB3 heterodimer functions as an oncogenic unit: ErbB2 requires ErbB3 to drive breast tumor cell proliferation. Proc Natl Acad Sci U S A 2003;100:8933–8.

27. Alroy I, Yarden Y. The ErbB signaling network in embryogenesis and oncogenesis: signal diversification through combinatorial ligand-receptor interactions. FEBS Lett 1997;410:83–6.

28. Gollamudi M, Nethery D, Liu J, Kern JA. Autocrine activation of ErbB2/ErbB3 receptor complex by NRG-1 in non-small cell lung cancer cell lines. Lung Cancer 2004;43:135–43.

29. Pinkas-Kramarski R, Soussan L, Waterman H, et al. Diversification of Neu differentiation factor and epidermal growth factor signaling by combinatorial receptor interactions. EMBO J 1996;15:2452–67.

30. Riese DJ II, van Raaij TM, Plowman GD, Andrews GC, Stern DF. The cellular response to neuregulins is governed by complex interactions of the erbB receptor family. Mol Cell Biol 1995;15:5770–6.

31. Tzahar E, Waterman H, Chen X, et al. A hierarchical network of interreceptor interactions determines signal transduction by Neu differentiation factor/neuregulin and epidermal growth factor. Mol Cell Biol 1996;16:5276–87.

32. Jaramillo ML, Leon Z, Grothe S, Paul-Roc B, Abulrob A, O'Connor McCourt M. Effect of the anti-receptor ligand-blocking 225 monoclonal antibody on EGF receptor endocytosis and sorting. Exp Cell Res 2006;312:2778–90.

33. Wiley HS. Trafficking of the ErbB receptors and its influence on signaling. Exp Cell Res 2003;284:78–88.

34. Waterman H, Sabanai I, Geiger B, Yarden Y. Alternative intracellular routing of ErbB receptors may determine signaling potency. J Biol Chem 1998;273:13819–27.

35. Rain TG, Ethier SP. Phosphatidylinositol 3-kinase recruitment by p185erbB-2

and erbB-3 is potently induced by neu differentiation factor/heregulin during mitogenesis and is constitutively elevated in growth factor-independent breast carcinoma cells with c-erbB-2 gene amplification. Cell Growth Differ 1996;7:551 - 61.

36. Cantley LC, Auger KR, Carpenter C, et al. Oncogenes and signal transduction. Cell 1991;64:281 - 302.

37. Engelman JA, Janne PA, Mermel C, et al. ErbB-3 mediates phosphoinositide 3-kinase activity in gefitinib-sensitive non-small cell lung cancer cell lines. Proc Natl Acad Sci U S A 2005;102:3788 - 93.

38. Kim HH, Sierke SL, Koland JG. Epidermal growth factor-dependent association of phosphatidylinositol 3-kinase with the erbB3 gene product. J Biol Chem 1994;269:24747 - 55.

39. Fiddes RJ, Janes PW, Sivertsen SP, Sutherland RL, Musgrove EA, Daly RJ. Inhibition of the MAP kinase cascade blocks heregulin-induced cell cycle progression in T-47D human breast cancer cells. Oncogene 1998;16:2803 - 13.

40. Vijapurkar U, Kim MS, Koland JG. Roles of mitogen-activated protein kinase and phosphoinositide 3′-kinase in ErbB2/ErbB3 coreceptor-mediated heregulin signaling. Exp Cell Res 2003;284:291 - 302.

41. Murphy LO, Smith S, Chen RH, Fingar DC, Blenis J. Molecular interpretation of ERK signal duration by immediate early gene products. Nat Cell Biol 2002;4:556 - 64.

42. Weber JD, Raben DM, Phillips PJ, Baldassare JJ. Sustained activation of extracellular-signal-regulated kinase 1 (ERK1) is required for the continued expression of cyclin D1 in G_1 phase. Biochem J 1997;326:61 - 8.

43. Yamamoto T, Ebisuya M, Ashida F, Okamoto K, Yonehara S, Nishida E. Continuous ERK activation down-regulates antiproliferative genes throughout G_1 phase to allow cell-cycle progression. Curr Biol 2006;16:1171 - 82.

44. Meloche S, Seuwen K, Pages G, Pouyssegur J. Biphasic and synergistic activation of p44mapk (ERK1) by growth factors: correlation between late phase activation and mitogenicity. Mol Endocrinol 1992;6:845 - 54.

45. Torii S, Yamamoto T, Tsuchiya Y, Nishida E. ERK MAP kinase in G cell cycle progression and cancer. Cancer Sci 2006;97:697 - 702.

46. Carter P, Smith L, Ryan M. Identification and validation of cell surface antigens for antibody targeting in oncology. Endocr Relat Cancer 2004;11:659 - 87.

47. Anido J, Matar P, Albanell J, et al. ZD1839, a specific epidermal growth factor receptor (EGFR) tyrosine kinase inhibitor, induces the formation of inactive EGFR/HER2 and EGFR/HER3 heterodimers and prevents heregulin signaling in HER2-overexpressing breast cancer cells. Clin Cancer Res 2003;9:1274 - 83.

48. Hu YP, Venkateswarlu S, Sengupta N, et al. Reorganization of ErbB family and cell survival signaling following knockdown of ErbB2 in colon cancer cells. J Biol Chem 2005;280:27383 - 92.

49. Funakoshi E, Hori T, Haraguchi T, et al. Overexpression of the human MNB/DYRK1A gene induces formation of multinucleate cells through overduplication of the centrosome. BMC Cell Biol 2003;4:12.

HUMAN MUTATION 28(6), 622–629, 2007

RESEARCH ARTICLE

Impact of Mutant p53 Functional Properties on *TP53* Mutation Patterns and Tumor Phenotype: Lessons from Recent Developments in the IARC TP53 Database

Audrey Petitjean,[1] Ewy Mathe,[1,2] Shunsuke Kato,[3] Chikashi Ishioka,[3] Sean V. Tavtigian,[4] Pierre Hainaut,[1]* and Magali Olivier[1]

[1]*Group of Molecular Carcinogenesis and Biomarkers, International Agency for Research on Cancer (IARC), World Health Organization, Lyon, France;* [2]*Laboratory of Human Carcinogenesis, National Cancer Institute, National Institutes of Health, Bethesda, Maryland;* [3]*Department of Clinical Oncology, Institute of Development Aging and Cancer, Aoba-ku Sendai, Japan;* [4]*Genetic Susceptibility Group, Genetics and Epidemiology Cluster, International Agency for Research on Cancer, World Health Organization, Lyon, France*

Communicated by David Goldgar

The tumor suppressor gene *TP53* is frequently mutated in human cancers. More than 75% of all mutations are missense substitutions that have been extensively analyzed in various yeast and human cell assays. The International Agency for Research on Cancer (IARC) *TP53* database (www-p53.iarc.fr) compiles all genetic variations that have been reported in *TP53*. Here, we present recent database developments that include new annotations on the functional properties of mutant proteins, and we perform a systematic analysis of the database to determine the functional properties that contribute to the occurrence of mutational "hotspots" in different cancer types and to the phenotype of tumors. This analysis showed that loss of transactivation capacity is a key factor for the selection of missense mutations, and that difference in mutation frequencies is closely related to nucleotide substitution rates along *TP53* coding sequence. An interesting new finding is that in patients with an inherited missense mutation, the age at onset of tumors was related to the functional severity of the mutation, mutations with total loss of transactivation activity being associated with earlier cancer onset compared to mutations that retain partial transactivation capacity. Furthermore, 80% of the most common mutants show a capacity to exert dominant-negative effect (DNE) over wild-type p53, compared to only 45% of the less frequent mutants studied, suggesting that DNE may play a role in shaping mutation patterns. These results provide new insights into the factors that shape mutation patterns and influence mutation phenotype, which may have clinical interest. Hum Mutat 28(6), 622–629, 2007. Published 2007 Wiley-Liss, Inc.†

KEY WORDS: TP53; p53; missense mutation; transactivation; functional assay

INTRODUCTION

The tumor suppressor gene *TP53* (OMIM #191117) encodes a transcription factor that responds to several forms of cellular stress and exerts multiple, antiproliferative functions [Vogelstein et al., 2000]. Somatic *TP53* gene alterations are frequent in most human cancers [Hainaut and Hollstein, 2000], ranging from 5 to 80% depending on the type, stage, and etiology of tumors. Inherited *TP53* mutations predispose to a wide spectrum of early-onset cancers and are associated with Li-Fraumeni and Li-Fraumeni-like syndrome (LFS and LFL, respectively) [Malkin et al., 1990].

Over the last 10 years, a great amount of systematic data has been generated on the functional impact of *TP53* missense mutations (single amino-acid substitutions), which are the most alterations observed in cancers (75%). Experimental assays have been performed in yeast and human cells to measure various properties including: 1) transactivation activities (TAs) of mutant proteins on reporter genes placed under the control of various p53 response-elements (p53-RE); 2) capacity of mutant proteins to induce cell-cycle arrest or apoptosis; 3) ability to exert dominant-negative effect (DNE) over the wild-type protein; 4) temperature sensitivity (TS) of mutant; and 5) activities of mutant proteins that are independent and unrelated to the wild-type protein (gain of function [GOF]). TA is the most studied functional property

The Supplementary Material referred to in this article can be accessed at http://www.interscience.wiley.com/jpages/1059-7794/suppmat.

Received 15 November 2006; accepted revised manuscript 12 January 2007.

*Correspondence to: Pierre Hainaut, Group of Molecular Carcinogenesis and Biomarkers, International Agency for Research on Cancer, World Health Organization, 150 Cours Albert Thomas, 69372 Lyon cedex 08, France. E-mail: Hainaut@iarc.fr

DOI 10.1002/humu.20495
Published online 20 February 2007 in Wiley InterScience (www.interscience.wiley.com).

and a single study has performed a systematic analysis of the activity of all possible missense mutations produced by single-nucleotide substitution in the entire sequence of *TP53* (2,314 mutations) on eight different p53-RE in yeast cells [Kato et al., 2003]. The study demonstrated that a great proportion of missense mutations retain partial TA on at least one promoter and that there is an overall good correlation between complete loss of TA and frequent occurrence in cancer.

Somatic and germline *TP53* mutations that are reported in the scientific literature are compiled in the IARC *TP53* Database (www-p53.iarc.fr). This database provides structured data and analysis tools to study mutation patterns in human cancers and cell-lines and to investigate the clinical impact of mutations. It contains annotations related to the clinical and pathological characteristics of tumors, as well as the demographics and carcinogen exposure of patients [Olivier et al., 2002]. Recently, new annotations and experimental data on the functional properties of mutant p53 proteins have been integrated in this database and new tools have been implemented to visualize these data and analyze mutation frequencies in relation to their functional impact and intrinsic nucleotide substitution rates. Here we present these developments and perform a systematic analysis of the database to identify the factors that shape the patterns and influence the phenotype of missense mutations in human cancers.

MATERIALS AND METHODS

Database Contents and Website

The information compiled in the IARC *TP53* database, and previously described in Olivier et al. [2002], has been reorganized in a single database maintained in an SQL server. Recent developments and database functionalities are described in details in the supplementary material (Supplementary Appendix S1, which includes Supplementary Figs. S1–S4; available online at http://www.interscience.wiley.com/jpages/1059-7794/suppmat). Among these developments, a new dataset that compiles data on functional activities and properties of p53 mutants has been integrated, and a web-based tool has been implemented to search and retrieve these data. Functional classifications have been derived from these data (see below).

Mutation Data

Data from the R10 release (July 2005) of the IARC TP53 Database, with updated information for the germline and function datasets (extracted from papers published in 2005), were used. For somatic mutations, only missense mutations detected by DNA sequencing in tumor samples (data from cell-lines or noncancerous tissues were excluded), and mutations located within exons 5 to 8 (most studies have screened only these exons) were included. For germline mutations, only tumors in individuals that have been screened for *TP53* mutation and identified as a mutation carrier were included.

Mutation Rates

Nucleotide substitution rates for each possible single-nucleotide substitution in the coding sequence of p53 have been calculated using a TP53 cDNA sequence (*Homo sapiens*|gi:35213) and dinucleotide substitution rates derived from human-mouse aligned sequence of chromosomes 21 and 10 [Lunter and Hein, 2004]. Mutation rates for single-nucleotide substitutions were calculated by averaging the dinucleotide substitution rates at that position for the forward and reverse strands. Amino-acid substitution rates were then calculated by summing up the rates of all possible nucleotide substitutions that lead to the desired amino-acid substitution. These rates are for germline mutations and we can not be sure that they apply to somatic mutations. However, they provide a reference rate that takes into account the sequence context.

Functional Classifications of Mutations

TA. TA were measured on eight p53-RE in yeast assays by Kato et al. [2003]. These measurements, expressed as percent of the wild-type protein, were used to classify mutants as "supertrans" (median TA on eight p53-RE above 140%), "functional" (median TA above 75% and below or equal to 140% of wild-type), "partially functional" (median TA above 20% and below or equal to 75%), and "nonfunctional" (median TA below or equal to 20%).

Conservation. All possible missense mutations were also systematically classified as "deleterious" or "neutral" by two different methods (SIFT [http://blocks.fhcrc.org/sift/SIFT.html] and Align-GVGD [http://agvgd.iarc.fr]) based on interspecies sequence conservation [Mathe et al., 2006].

DNE over wild-type p53. A list of 117 mutants was selected from the "Function" dataset based on the following criteria: 1) mutants located within exons 5–8 and with available DNE status on both *WAF1* and *RGC* promoters (these promoters were the most frequently used in different studies to assess DNE status); 2) mutants from a large systematic study by Dearth et al. [2007] that included 76 mutants. Mutants were classified as "DNE" if they were DN on both *WAF1* and *RGC* promoters, or on all promoters in the large study, "moderate-DNE" if they were DN on some promoters and not on others, and "non-DNE" if they were not DN on both *WAF1* and *RGC* promoters, or none of the promoters in the large study. Of 117 mutants, 39 were classified "non-DNE," 18 "moderate-DNE," and 60 "DNE."

RESULTS AND DISCUSSION

Transcriptional Activities, Mutation Rates, and Frequency of Mutations in Sporadic Cancers

The majority (75%) of mutations reported in the database are missense substitutions that show a great variability in their type and position, with over 260 distinct mutations frequently reported in human sporadic cancers. All possible missense mutations obtained by single-nucleotide substitution along the full coding sequence of *TP53*, named MSS hereafter, were classified as "supertrans," "functional," "partially functional," and "nonfunctional" based on experimental measurements obtained by Kato et al. [2003] in yeast assays (see Materials and Methods). Of all MSS located within exons 5–8 (1,070 mutants), 31% (334) were "functional," 27% (288) were "partially functional," 4% (46) were "supertrans," and 38% (402) were "nonfunctional." In contrast, only 15% (23/156) of the corresponding mutants that have never been reported in human cancers were nonfunctional, while 41% (376/902) of distinct mutants and 81% (9821/12153) of all mutants reported in cancer were nonfunctional. This indicates a strong selection for loss of TA during cancer development.

When mutants were grouped according to their frequency in cancer, nine nonfunctional mutants accounted for 31% of all observed MSS, while 795 mutants, of which more than 65% retained some transactivation activity, represented 32% of observed MSS (Fig. 1A). Thus, mutants that are rarely reported in cancer are more likely to retain some transactivation activity. Many of these may represent by-stander mutations that were not selected for their loss of function, and some may represent sequencing errors.

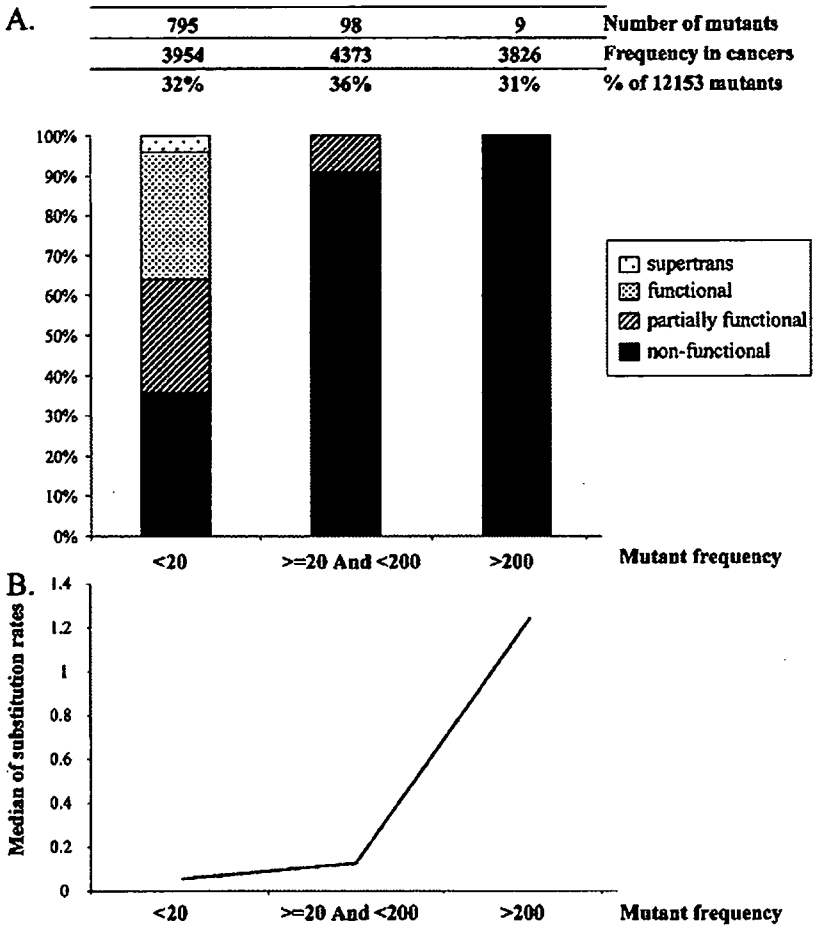

FIGURE 1. **Transactivation capacity, mutation rates, and frequency in cancer. A: Distribution of the different TA classes of mutants according to their frequency in the somatic dataset of the IARC *TP53* database (R10, July 2005). Three groups have been defined: above 200 occurrences, between 200 and 20 occurrences, and below 20 occurrences. The number of mutants and the corresponding number of entries in the database are indicated. Only mutations detected by DNA sequencing and located within the DNA-binding domain were included. B: Median mutation rates of corresponding mutants in the three different frequency groups.**

The proportion of functional and nonfunctional mutants varied from one cancer to the other. Table 1 shows the proportions of nonfunctional mutants in various types of cancers compared to CRC. Colorectal cancer was chosen as a reference because it presented the highest frequency of hotspot mutants. The highest proportion of nonfunctional mutants was observed in ovarian carcinomas (92.0% vs. 84.9% for CRC; $p < 0.005$), suggesting a strong selection for loss of transactivation in this type of cancer. In contrast, in cervical cancer, there were significantly fewer nonfunctional mutants than in CRC (62.1% vs. 85% for CRC; $p < 0.0001$). The main etiology of cervical cancer is human papilloma virus (HPV), which produces the E6 protein that inactivates p53 by protein–protein interaction. Thus, HPV infection decreases the selection pressure for loss of p53 function by gene mutation. Indeed, *TP53* gene mutations are infrequent (about 5%) in cervical cancers. Among cases carrying a *TP53* mutation, a subset of 46 cervical cancers had documented HPV status. In HPV-positive cases, a lower proportion of nonfunctional mutants (36.4%; 5/22) was found, compared to HPV-negative cases (70.8%; 17/24). Thus, the presence of the virus may also decrease the selection pressure for mutations with loss of TA. A lower frequency (below 75%) of nonfunctional mutations was also found in oral squamous cell carcinomas (SCC), prostate cancers, and nonmelanoma skin cancers (Table 1). Since HPV is also a risk factor for oral and skin SCC, it is possible that a proportion of these cancers with functional mutations are linked to HPV. In fact, in a subset of 41 oral SCC with documented HPV status in the database, 80.6% (25/31) of HPV-negative cases had nonfunctional mutations in contrast to 60% (6/10) of HPV-positive cases. In prostate cancer, whose etiology is poorly understood, 72.2% (109/151) had nonfunctional mutants. It would be interesting to confirm this finding in a larger dataset and investigate the reason of a lower selection pressure for loss of TA.

The median nucleotide substitution rates of mutants grouped according to their frequency in the database are shown in Figure 1B. These rates reflect the propensity of each mutation to occur as a neutral process from replication error or endogenous mutagenesis (see Materials and Methods). The group of rare mutants had the lowest median nucleotide substitution rates while the group of most frequent mutants had the highest rates, indicating that underlying substitution rates play a major role in determining mutation frequency. Transitions at CpG sites have the highest mutation rates, thus are expected to be the most frequently observed mutations. However, only 7 out of 34 transitions at CpG sites within the DNA-binding domain are frequently observed in cancers. The median TA of the seven frequent mutants is below

TABLE 1. Transactivation Activities by Cancer Type for Mutations Localized in the DNA Binding Domain

Cancer type[a]	Nonfunctional[b]	Others	Dataset size[c]	RR (95%CI)[d]
CRC	1568 (84.9%)	279 (15.1%)	1847	1 (reference)
Oral SSC	327 (70.5%)	137 (29.5%)	464	0.83 (0.78–0.88)*
Larynx SCC	114 (81.4%)	26 (18.6%)	140	0.96 (0.88–1.04)
Lung NSCC	841 (81.0%)	197 (19.0%)	1038	0.95 (0.92–0.99)*
Esophagus SCC	543 (80.1%)	135 (19.9%)	678	0.94 (0.90–0.98)*
Esophagus ADC	143 (85.6%)	24 (14.4%)	167	1.01 (0.95–1.08)
Stomach ADC	135 (75.8%)	43 (24.2%)	178	0.89 (0.82–0.97)*
Liver HCC	394 (86.2%)	63 (13.8%)	457	1.02 (0.97–1.06)
Bladder TCC	229 (79.2%)	60 (20.8%)	289	0.93 (0.88–0.99)*
Prostate	109 (72.2%)	42 (27.8%)	151	0.85 (0.77–0.94)*
Brain gliomas	784 (86.4%)	123 (13.6%)	907	1.02 (0.99–1.05)
Breast	896 (80.0%)	224 (20.0%)	1120	0.94 (0.91–0.98)*
Cervix	46 (62.1%)	28 (37.9%)	74	0.73 (0.61–0.88)*
Ovary carcinomas	208 (92.0%)	18 (8.0%)	226	1.08 (1.04–1.13)
Lymphoïd leukemias	141 (81.0%)	33 (19.0%)	174	0.95 (0.89–1.03)
Myeloïd leukemias	73 (85.9%)	12 (14.1%)	85	1.01 (0.93–1.11)
Mature B-cell lymphomas	204 (79.4%)	53 (20.6%)	257	0.94 (0.88–1.00)
Skin BCC	123 (69.1%)	55 (30.9%)	178	0.81 (0.74–0.90)*
Skin SCC	80 (66.7%)	40 (33.3%)	120	0.79 (0.69–0.89)*

[a]No significant difference was observed between colorectal cancer and larynx SCC, lung SmCC, esophagus ADC, pancreas ADC, liver HCC, leukemias and osteosarcomas.
[b]Categories of mutants based on their transactivation activities as defined in Materials and Methods. Only mutations located in the DNA binding domain were included to avoid the bias due to the fact that most studies have analyzed only this region.
[c]Tumor samples with the indicated topography and morphology were selected where mutation was detected in DNA and exons 5–8 were screened. Cell-lines were excluded.
[d]Univariate analysis of RR with CRC as reference. CRC was used as a reference group because it recapitulates the overall spectrum of missense mutations.
*Statistically significant difference with reference.
ADC, adenocarcinoma; BCC, basal cell carcinoma; CRC, colorectal cancer; HCC, hepatocellular carcinoma; NSCC, non-small-cell carcinoma; SCC, squamous cell carcinoma; TCC, transitional cell carcinoma; RR, relative risk; CI, confidence interval.

10% (median TA of seven mutants is 0), whereas it is between 15% and 140% for 24 out of the 27 rare mutants (median TA of mutants is 55.6) (Supplementary Table S1). Thus, residual TA is likely to be responsible for the counter-selection of these 24 mutants. Three mutants with a median TA < 10% (R213Q, R267W, and R283H) were among the rare mutants. R267W retain significant activity on two promoters (40% for Gadd45 and 85% for P53R2), R213Q has been shown to retain TA on *MDM2* and growth suppressive activity in human cells [Hsiao et al., 1994; Pan and Haines, 2000], and R283H to retain apoptotic activity in Saos-2 cells and TA on *WAF1* in yeast assays [Maurici et al., 2001; Smith et al., 1999]. Thus, these mutants may retain some activities that would be sufficient for their counter-selection in cancer.

Transcriptional Activity and Phenotype of Germline Mutations

TP53 germline mutations are associated with LFS and LFL syndromes [Olivier et al., 2003]. The clinical definition of LFS includes a proband with early-onset sarcoma and a first-degree relative with cancer at <45 years of age plus another first- or second-degree relative with cancer at <45 years of age or sarcoma at any age. Different definitions are used for LFL, which correspond to extended definitions of LFS (including sarcomas at any age, or other childhood cancers in probands). *TP53* germline mutations have also been reported in individuals with no family history (noFH) or with a family history (FH) not fulfilling LFS of LFL definitions. LFS corresponds to the more severe phenotype since it includes three tumors at <45 years, whereas LFL definitions include one or two tumors at any age, and FH usually corresponds to familial clustering of tumors with later onset cancers [Olivier et al., 2003]. In cancer families carrying a *TP53* germline mutation, of the 238 missense mutations reported in the database, 73% were nonfunctional, 7% functional, and 20% retained various degrees of TA. The most frequent cancers associated with *TP53* mutations are breast cancer (BC), bone and soft tissue sarcomas (BoneS and STS), brain tumors (BT), and adrenocortical carcinomas (ADR) [Olivier et al., 2003; Wong et al., 2006]. Other less frequent cancers include leukemias, stomach cancer, colorectal cancer [Birch et al., 2001]. Of the 78 missense mutations reported in LFS families, 92% were nonfunctional, compared to 70% for LFL (42/60), 65% for FH (26/40), and 51% (25/49) for noFH. Thus, there was a striking relation between the proportion of nonfunctional mutants and family history, suggesting that the severity of a mutation phenotype is related to its functional activity. To further investigate this hypothesis, the mean age at onset of tumors in confirmed carriers of missense mutations was compared between functional and nonfunctional missense mutations for cancers where at least four tumors with age data was available. The mean age at onset in carriers of a functional mutation was higher than the one for carriers of a nonfunctional mutation for several cancers. For example, breast and colorectal cancers show a difference of more than 10 years (Table 2). Thus, the penetrance of a mutation may be related to its degree of loss of TA. The fact that transcription-competent mutations were found in cancer families was surprising. Among these families, 7 out of 20 carried a mutation that were predicted deleterious based on sequence conservation [Mathe et al., 2006]. It is thus possible that loss of an activity independent of TA, or not captured by the assay measuring TA, contributes to the observed phenotypes. In one family, the *TP53* mutation (N210Y) was concomitant with a truncating mutation in *APC* [Zajac et al., 2000]. The phenotype in this family was classical familial adenomatous polyposis syndrome (FAP; associated with *APC* mutation) but with a more severe phenotype than expected from the associated *APC* mutation. This example shows how a combination of mutations with intermediate penetrance in two tumor suppressor genes may result in atypical phenotypes.

Gain of Function and Occurrence in Cancer

In addition to loss of transactivation, the acquisition of new properties by p53 mutants resulting in oncogenic activities (gain of function [GOF]), has also been proposed to play a major role in the selection of mutations. Various GOF properties have been described, including the activation of genes normally unaffected or repressed by wild-type p53, interference with other transcription factors, and resistance to specific drugs. Analysis of this information showed that most data on these properties were obtained on hotspot mutants (Supplementary Table S2) and that no large systematic study has been performed that would allow a systematic analysis of cancer-related mutants toward their GOF properties. Despite these limitations, three categories of GOF have been selected, where data were available for more than 50 distinct mutants and for more than 70 experiments measuring: 1) interference with p73 activity; 2) transactivation of genes repressed by wild-type p53; and 3) cooperation with oncogene for transformation of rat embryonic fibroblast (REF) or mouse embryonic fibroblast (MEF) cells (Supplementary Table S2). Using these three categories, we were unable to establish any link between GOF and the frequency of p53 mutants reported in sporadic cancers. For example, R175H, which is the most frequently reported mutant (reported 944 times), has GOF properties in all categories. However, two rare (reported less than 20 times) mutants, V143A and D281G, have also been shown to have GOF properties in the three categories. In fact, the more frequently a mutant is reported in cancer, the more it was studied for functional properties and the more likely it is to exhibit a GOF (Supplementary Table S2).

Studies in mouse models of LFS have reported evidence of GOF for R175H and R273H mutants [Lang et al., 2004; Olive et al., 2004]. Tumors in these knock-in mice were more metastatic or were arising in different tissues compared to knock-out mice. Interference with p63/73 and increased cell proliferation was suggested to be the underlying molecular mechanism. In the database, 30 mutants that have been reported in the germline could be classified according to the three GOF categories defined above. Only one mutant was negative for p73 interference, while all other mutants were positive for GOF in at least one category. Thus, we could not determine if there was any difference in tumor spectrum or age at onset between mutants with and without GOF activities.

TABLE 2. Mean Age at Onset of Cancers in Relation to Transactivation Property of Germline *TP53* Mutations*

Tumor site/type	Nonfunctional	Functional/partially functional
Breast carcinoma	33.6	43.2
Soft tissue sarcoma	17.4	22.5
Brain tumor	23.9	29.9
Bone sarcoma	16.9	17.7
Adrenocortical carcinoma	3.2	6.6
Lung carcinoma	46.1	48.8
Colorectal carcinoma	36.3	52.0

*Tumors in confirmed-carriers of a germline *TP53* mutation reported in the IARC TP53 Database (R10, July 2005).

DNE and Occurrence in Cancer

P53 transcriptional activity relies on the formation of tetramers (dimers of dimers). Mutant proteins may interfere with wild-type p53 by forming heterooligomers less competent for specific DNA-binding. The capacity of mutant proteins to interfere with the wild-type form has been studied in yeast and human cell assays in various settings. The first systematic study was performed in yeast, and measured the ability of 35 mutants to inhibit the TA of wild-type p53 on its consensus response-element [Brachmann et al., 1996]. It showed that DNE property correlated with occurrence in cancer. Since then, data has been produced on more than 200 mutants and it appears that DNE is promoter- and cell-type-dependent [Dearth et al., 2007].

A group of 117 mutants that were tested for DNE with comparable methods (see Materials and Methods) was selected for

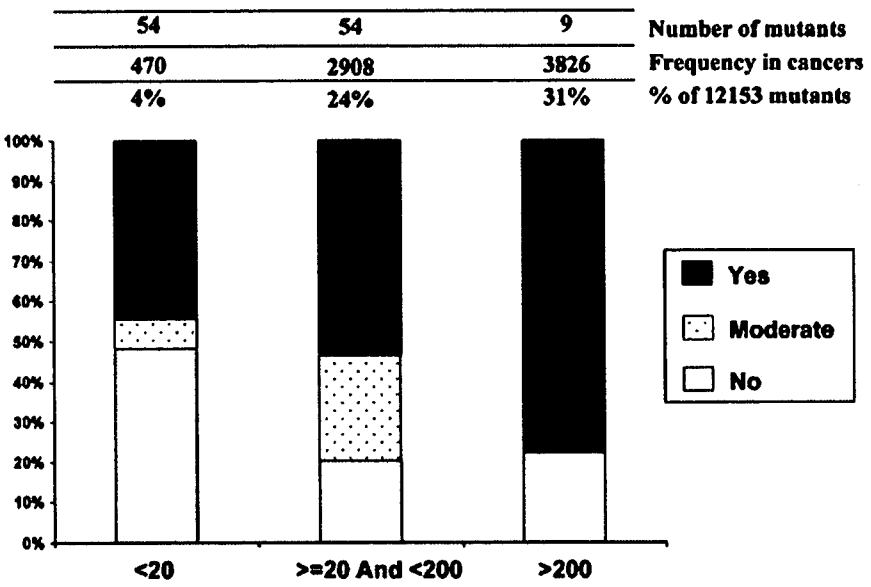

FIGURE 2. Dominant-negative property and frequency of missense mutants in cancer. Distribution of the different DNE classes of mutants according to their frequency in the somatic dataset of the IARC *TP53* database (R10, July 2005). The number of mutants with available DNE data and the corresponding number of entries in the database are indicated. Only cancer mutants detected by DNA sequencing and located within the DNA-binding domain were included.

database analysis. As shown in Figure 2, the proportion of DNE mutants was correlated with frequency of occurrence of sporadic cancers, 80% of the nine hotspot mutants being DNE. Moreover, the proportion of DNE mutants among the nonfunctional mutants was lower in the category of less frequent mutants (67.6% in the "<20" category compared to 80% in the frequency categories "20–200" and ">200"). Thus, DNE may also contribute to the selection of mutants in sporadic cancers. However, to thoroughly assess the role of DNE in cancer development, one would need to know the status of loss of heterozygosity (LOH) in the tumor, a question that is rarely addressed in original studies and therefore poorly documented in the database.

In a subgroup of 121 nonfunctional germline mutations classified for dominant-negative activities, 82.6% were DNE or moderate-DNE. While the age at onset of tumors associated with DNE and non-DNE mutants was similar, the type of tumors showed some differences. Bone sarcomas were half as frequent in carriers of DNE mutants compared to carriers of non-DNE mutants (odds ratio [OR] = 0.45; 95% confidence interval [95%CI] = 0.21–0.96; p = 0.023) and breast cancers were twice more frequent in carriers of DNE mutants compared to carriers of non-DNE mutants (OR = 2.21; 95%CI = 0.84–6.09; p = 0.079). In tumors from carriers of DNE mutants, LOH would be expected to be very low. However, in LFS families, LOH has been shown to occur in about half of the tumors [Varley et al., 1997]. As in sporadic cancers, it would be necessary to perform systematic assessment of LOH in tumor samples from carriers of mutations with different DNE properties to clearly established whether and how DNE may influence tumor development.

Hotspots and Cancer Type

Figure 3 shows a scatterplot graph that display mutants according to their frequencies, nucleotide substitution rates and functional impact (based on TA). Missense mutations with TA similar to wild-type p53 (functional) are close to the y-axes, indicating a very low frequency, even for mutations with high substitution rates. In contrast, the frequency of missense mutations with complete loss of TA (nonfunctional) increased with substitution rates. This type of graph was used to identify the most frequent mutants in specific cancer types (Table 3). R175H, R248Q, R248W, and R273H are the most frequent mutants in many cancers, except lung, larynx, bladder, liver, and skin carcinomas. In these latter cancers, hotspots have been linked to the exposure to environmental factors: tobacco smoke for lung cancer, tobacco smoke and alcohol for head and neck cancers, aromatic-amines for bladder cancer, aflatoxine-B1 and hepatitis B virus (HBV) in liver cancer, and ultraviolet (UV) rays in skin cancer [reviewed in Olivier et al., 2004]. In lung cancers, V157F, R158L, R248L, and R273L hotspots are due to G>T transversions that have been shown to be caused by the presence of benzo(a)-pyrene diol epoxide (BPDE) adducts on guanines at these codons [Denissenko et al., 1996]. BPDE is the main metabolite of benzo(a)-pyrene, one of the most potent carcinogens present in high quantity in tobacco smoke. In lung tissue from smokers, the actual nucleotide substitution rate for these mutants is thus expected to be higher than the one estimated from endogenous processes. These hotspots are all defective for TA with less than 20% of wild-type activity on all p53-RE (colored in red

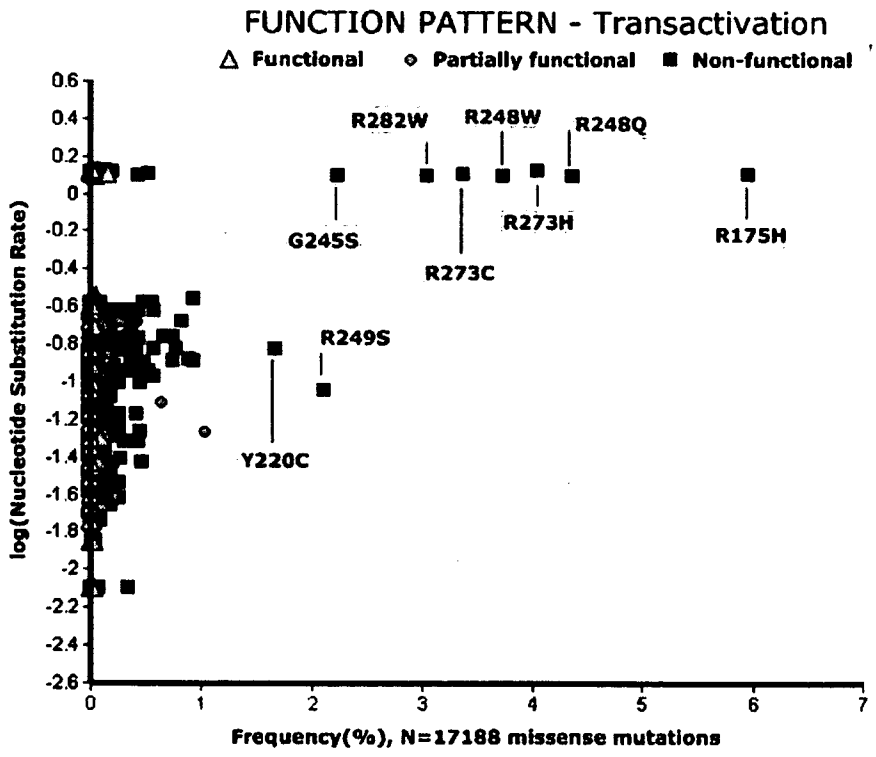

FIGURE 3. **Interactive scatter plot graph. This graph depicts the frequency (x-axis) of single amino-acid substitutions in relation to their observed functional impacts (TA) and nucleotide substitution rates (y-axis in log). Each point represents a single amino-acid substitution that is shaped and colored according to the TA capacity of the mutation (green, functional; blue, partially functional; red, nonfunctional). On the website, the points can be clicked to obtain all information available in the database for the selected mutation.**

TABLE 3. Most Frequent Missense Mutants Observed in Specific Cancer Types

Cancer type	Dataset size[a]	Hotspots[b]
CRC	1847	R175H > R248W-R282W-R248Q-R273H-G245S-R273C
Oral SSC	464	R248Q-R175H-R273C-R282W
Larynx SCC	140	**V157F** > R175H-R273C-R273H-**R248L-C176F**-Y220C
Lung NSCC	1038	**R158L-V157F-R249S-R273L-R249M-R248L**
Esophagus SCC	678	**C176F**-R175H-R282W-R273H-R248W-R248Q
Esophagus ADC	167	R175H-R248W-R273H-R282W-G245S-R248Q
Stomach ADC	178	R175H-R282W-R248Q-R248W-R273C-G245S-R273H
Liver HCC	457	**R249S**
BladderTCC	289	R248Q-**E285K**-R282W-R175H-Y220C
Prostate	151	R273C
Brain gliomas	907	R273C > R175H-R248Q-R273H-R248W-R282W
Breast	1120	R175H-R248Q-R273H-R248W
Cervix	74	R248Q-R273C-R175H
Ovary carcinomas	226	R273H-R175H-R248W-H179R-R248Q-R273C-G245S
Lymphoid leukemias	174	R175H-R248Q-R273H
Myeloid leukemias	85	R248Q-R273C-R175H
Mature B-cell lymphomas	257	R248Q-R175H-R248W-R273H-R273C
Skin BCC	178	**H179Y**-R248W-**R272W-P177L-S241F**
Skin SCC	120	R248W-R282W-**H179Y**

[a]Number of entries for missense mutations in the selected cancers in the IARC TP53 Database (R10, July 2005).
[b]Most frequent mutants in each cancer. Mutants that are cancer-specific hotspots are indicated in bold.
ADC, adenocarcinoma; BCC, basal cell carcinoma; HCC, hepatocellular carcinoma; NSCC, non-small-cell carcinoma; SCC, squamous cell carcinoma; TCC, transitional cell carcinoma.

on the graph). Another site of adduct formation by BPDE is the third base of codon 267, but the resulting mutation would not produce an amino-acid change. This mutation has been reported only once in a breast tumor sample. These results show that both mutagenesis and selection of loss of trans-activation is shaping the patterns of mutation observed in lung cancer. In other tissues where nonclassical hotspots are observed (in bold in Table 3), similar mechanisms involving other carcinogens or specific mutagenic conditions are suspected to be involved.

In brain and prostate cancers, the R273C mutant is more frequent than any other mutants (13% vs. 8% for R175H in brain, and 9% vs. 2.6% for R175H in prostate). Because the R273C mutant results from a transition at CpG site (high mutation rate) and is inactive for transactivation on all p53-RE, it would be expected to be more frequently observed in other cancer types. The reason why this mutant is preferentially selected in brain and prostate cancers while the R175H, R248Q/W, and R273H mutants are preferentially selected in other cancers is unclear. In one large systematic study in yeast, R273C has been shown to have moderate DNE while R175H, R248Q/W, and R273H had strong DNE [Dearth et al., 2007]. A less potent DNE may thus explain why this mutant is observed less frequently than expected, but the exception of brain and prostate cancers remains to be investigated.

CONCLUSION

The integration of standardized annotations on the functional impact of missense mutations in the IARC *TP53* database provides a powerful framework for the analysis of "functional" patterns of mutations in cancers and the detection of genotype/phenotype associations. Analyses of mutation patterns and phenotypes with these annotations showed that p53 missense mutation patterns are shaped by both underlying nucleotide substitution rates and functional selection, where selection is based mainly on loss of TA with possibly an additive role of DNE. Experimental data currently available on mutant GOF are still scarce and heterogeneous, and it thus remains unclear whether the acquisition of novel functional properties contributes to the selection of particular mutant or has an impact on tumor development. Nontranscriptional functions of wild-type p53, such as protein–protein interactions involved in apoptosis or DNA repair, that may be lost by mutant p53 could not be addressed because data were not available.

The central role of TA is underlined by the observation that this activity was related to the penetrance of germline *TP53* mutations, influencing in particular the age at diagnosis of several of tumors. Thus, this knowledge may have an impact on the management of germline mutation carriers. It is tempting to speculate that the same effect may also apply to the prognosis of tumors with somatic mutations. However, in a recent study on a large series of patients with breast cancer, we found that *TP53* mutations were an independent factor of poor prognosis [Olivier et al., 2006], but that TA did not accurately predict differences in survival among patients with *TP53* mutations. In contrast, we showed that mutations occurring at the DNA-binding surface and mutations precluding protein assembly (nonsense, frameshifts, and mutations at splice junctions) had a similar poor prognosis, while mutations occurring in loops and beta-strands that support the DNA-binding surface had a better prognosis. Thus, clinical observations indicate that somatic mutations are not all functionally equivalent, at least in breast cancer. However, it remains to be assessed whether the milder prognosis associated to several missense mutants may be ascribed to specific functional properties.

ACKNOWLEDGMENTS

We thank Lawrence R. Dearth and Rainer K. Brachmann for providing their functional data ahead of publication, and A. Inga and M. Resnick for submitting additional information to the database. We also thank S. Grant for her assistance in the collection of the literature and all authors who provided data and additional information, thus helping us to improve the quality of the annotations. The development of the IARC *TP53* database is funded by IARC and by EC FP6. This publication reflects the author's views and not necessarily those of the EC. The Community is not liable for any use that may be made of the information contained herein. A. Petitjean was supported by a Special Training Award from IARC, funded by the National Institute of Environmental Health Sciences (NIEHS).

REFERENCES

Birch JM, Alston RD, McNally RJ, Evans DG, Kelsey AM, Harris M, Eden OB, Varley JM. 2001. Relative frequency and morphology of cancers in carriers of germline TP53 mutations. Oncogene 20:4621–4628.

Brachmann RK, Vidal M, Boeke JD. 1996. Dominant-negative p53 mutations selected in yeast hit cancer hotspots. Proc Natl Acad Sci USA 93:4091–4095.

Dearth LR, Qian H, Wang T, Baroni TE, Zeng J, Chen SW, Yi SY, Brachmann RK. 2007. Inactive full-length p53 mutants lacking dominant wild-type p53 inhibition highlight loss-of-heterozygosity as an important aspect of p53 status in human cancers. Carcinogenesis 28:289–298.

Denissenko MF, Pao A, Tang M, Pfeifer GP. 1996. Preferential formation of benzo[a]pyrene adducts at lung cancer mutational hotspots in P53. Science 274:430–432.

Hainaut P, Hollstein M. 2000. p53 and human cancer: the first ten thousand mutations. Adv Cancer Res 77:81–137.

Hsiao M, Low J, Dorn E, Ku D, Pattengale P, Yeargin J, Haas M. 1994. Gain-of-function mutations of the p53 gene induce lymphohematopoietic metastatic potential and tissue invasiveness. Am J Pathol 145:702–714.

Kato S, Han SY, Liu W, Otsuka K, Shibata H, Kanamaru R, Ishioka C. 2003. Understanding the function-structure and function-mutation relationships of p53 tumor suppressor protein by high-resolution missense mutation analysis. Proc Natl Acad Sci USA 100:8424–8429.

Lang GA, Iwakuma T, Suh YA, Liu G, Rao VA, Parant JM, Valentin-Vega YA, Terzian T, Caldwell LC, Strong LC, El Naggar AK, Lozano G. 2004. Gain of function of a p53 hot spot mutation in a mouse model of Li-Fraumeni syndrome. Cell 119:861–872.

Lunter G, Hein J. 2004. A nucleotide substitution model with nearest-neighbour interactions. Bioinformatics 20(Suppl 1):I216–I223.

Malkin D, Li FP, Strong LC, Fraumeni JFJ, Nelson CE, Kim DH, Kassel J, Gryka MA, Bischoff FZ, Tainsky MA. 1990. Germ line p53 mutations in a familial syndrome of breast cancer, sarcomas, and other neoplasms. Science 250:1233–1238.

Mathe E, Olivier M, Kato S, Ishioka C, Hainaut P, Tavtigian SV. 2006. Computational approaches for predicting the biological effect of p53 missense mutations: a comparison of three sequence analysis based methods. Nucleic Acids Res 34:1317–1325.

Maurici D, Monti P, Campomenosi P, North S, Frebourg T, Fronza G, Hainaut P. 2001. Amifostine (WR2721) restores transcriptional activity of specific p53 mutant proteins in a yeast functional assay. Oncogene 20:3533–3540.

Olive KP, Tuveson DA, Ruhe ZC, Yin B, Willis NA, Bronson RT, Crowley D, Jacks T. 2004. Mutant p53 gain of function in two mouse models of Li-Fraumeni syndrome. Cell 119:847–860.

Olivier M, Eeles R, Hollstein M, Khan MA, Harris CC, Hainaut P. 2002. The IARC TP53 database: new online mutation analysis and recommendations to users. Hum Mutat 19:607–614.

Olivier M, Goldgar DE, Sodha N, Ohgaki H, Kleihues P, Hainaut P, Eeles RA. 2003. Li-Fraumeni and related syndromes: correlation between tumor type, family structure, and TP53 genotype. Cancer Res 63: 6643–6650.

Olivier M, Hussain SP, Caron dF, Hainaut P, Harris CC. 2004. TP53 mutation spectra and load: a tool for generating hypotheses on the etiology of cancer. IARC Sci Publ 157:247–270.

Olivier M, Langerod A, Carrieri P, Bergh J, Klaar S, Eyfjord J, Theillet C, Rodriguez C, Lidereau R, Bieche I, Varley J, Bignon Y, Uhrhammer N, Winqvist R, Jukkola-Vuorinen A, Niederacher D, Kato S, Ishioka C, Hainaut P, Borresen-Dale AL. 2006. The clinical value of somatic TP53 gene mutations in 1,794 patients with breast cancer. Clin Cancer Res 12: 1157–1167.

Pan Y, Haines DS. 2000. Identification of a tumor-derived p53 mutant with novel transactivating selectivity. Oncogene 19:3095–3100.

Smith PD, Crossland S, Parker G, Osin P, Brooks L, Waller J, Philp E, Crompton MR, Gusterson BA, Allday MJ, Crook T. 1999. Novel p53 mutants selected in BRCA-associated tumours which dissociate transformation suppression from other wild-type p53 functions. Oncogene 18:2451–2459.

Varley JM, Thorncroft M, McGown G, Appleby J, Kelsey AM, Tricker KJ, Evans DG, Birch JM. 1997. A detailed study of loss of heterozygosity on chromosome 17 in tumours from Li-Fraumeni patients carrying a mutation to the TP53 gene. Oncogene 14:865–871.

Vogelstein B, Lane D, Levine AJ. 2000. Surfing the p53 network. Nature 408:307–310.

Wong P, Verselis SJ, Garber JE, Schneider K, DiGianni L, Stockwell DH, Li FP, Syngal S. 2006. Prevalence of early onset colorectal cancer in 397 patients with classic Li-Fraumeni syndrome. Gastroenterology 130: 73–79.

Zajac V, Tomka M, Ilencikova D, Majek P, Stevurkova V, Kirchhoff T. 2000. A double germline mutations in the APC and p53 genes. Neoplasma 47:335–341.

Influence of histological type, smoking history and chemotherapy on survival after first-line therapy in patients with advanced non-small cell lung cancer

Toru Itaya,[1] Nobuyuki Yamaoto,[1,3] Masahiko Ando,[2] Masako Ebisawa,[1] Yukiko Nakamura,[1] Haruyasu Murakami,[1] Gyo Asai,[1] Masahiro Endo[1] and Toshiaki Takahashi[1]

[1]Thoracic Oncology Division, Shizuoka Cancer center, Shimonagakubo, Nagaizumi-cho, Sunto-gun, Shizuoka 411-8777; [2]Department of Preventive Services, Kyoto University School of Public Health, Kyoto 606-8507, Japan

(Received August 3, 2006/Revised September 20, 2006/Accepted October 2, 2006/Online publication December 13, 2006)

The usual primary endpoint in clinical trials for first-line chemotherapy in advanced non-small cell lung cancer is overall survival. Second-line chemotherapy can also prolong overall survival. Non-smoking history has been associated with a treatment effect for epidermal growth factor receptor-tyrosine kinase inhibitor (EGFR-TKI) versus placebo for overall survival. We performed a retrospective analysis to identify prognostic factors for progression-free survival and overall survival in patients with advanced non-small cell lung cancer treated with first-line carboplatin/paclitaxel, and to examine the effect of second-line therapy on progression-free survival and overall survival. Ninety-eight patients (median age 61 years, 35 female, 74 adenocarcinoma, 68 smokers, 56 performance status 0) fulfilled our criteria, of which 75 patients (78%) received more than second-line therapy (docetaxel [54%] gefitinib [48%] erlotinib [4%]). For overall survival, smoking history and histology were significant prognostic factors. The 2-year overall survival rates were as follows: smokers, 17%; non-smokers, 52%, $P < 0.0001$; adenocarcinoma, 40%; other 15%, $P = 0.0017$. Multivariate analysis in patients who received second-line therapy showed treatment with EGFR-TKI was an independent predictor of overall survival. Smoking history and adenocarcinoma histology were prognostic factors for an improved outcome with carboplatin/paclitaxel in patients with non-small cell lung cancer. Our study results suggest that the use of EGFR-TKI after first-line treatment may be associated with an improvement in overall survival. (*Cancer Sci* 2007; 98: 226–230)

Lung cancer is the malignant tumor with the highest mortality rates in the world.[1] Approximately 80% of all lung cancer cases are non-small cell lung cancer (NSCLC) and patients with postoperative recurrence or advanced NSCLC may be treated with systemic chemotherapy. Platinum-based chemotherapy is widely used as first-line treatment. Various combination regimens are available – the Four-Arm Cooperative Study (FACS) conducted in Japan between October 2000 and June 2002 did not demonstrate any superiority of three experimental platinum-based regimens (cisplatin/gemcitabine, cisplatin/vinorelbine and carboplatin/paclitaxel) compared with the reference arm of cisplatin/irinotecan.[2,3] However, due to its good tolerability, ease of use and experience in Western countries, carboplatin/paclitaxel is currently the standard first-line chemotherapy for NSCLC in Japan.

Docetaxel has been widely used as second-line therapy for NSCLC in Japan. However, since its approval in July 2002, the use of gefitinib (IRESSA), an epidermal growth factor receptor tyrosine kinase inhibitor (EGFR-TKI), has been increasing each year. Erlotinib, another EGFR-TKI, which is approved in a number of Western markets has also been used in clinical registration trials in some Japanese medical institutions. Gefitinib was the first molecular targeted agent to be approved for the treatment of NSCLC in Japan. Two international cooperative Phase II studies (IRESSA Dose Evaluation in Advanced Lung Cancer Trial: IDEAL1 and 2) demonstrated efficacy (response rates, 12.0–18.9%) and favorable tolerability of gefitinib in the treatment of NSCLC after failure of platinum-based chemotherapy.[4,5] Furthermore, the results of subset analyses of IDEAL1 indicated that the patient characteristics of Japanese nationality, female gender and adenocarcinoma histology were associated with longer overall survival (OS).[4]

In a placebo-controlled Phase III study (BR21) erlotinib significantly prolonged OS compared with placebo in patients with previously treated NSCLC.[6] A similar Phase III study (IRESSA Survival Evaluation in Lung Cancer [ISEL]) of gefitinib in refractory, advanced NSCLC showed an improvement in survival compared with placebo in the overall study population, which did not reach statistical significance.[7] However, in a subset analysis, statistically significantly longer survival was demonstrated in patients of Asian origin and in patients who had never smoked.[7] With the availability of new second-line anticancer agents such as gefitinib and erlotinib, it is necessary to consider more fully the influence of second-line treatment on evaluation of OS following standard first-line treatment. Since the opening of our department in October 2002, carboplatin/paclitaxel has been used as the standard first-line therapy for NSCLC, while the use of gefitinib as second-line therapy is increasing each year. In this study we performed retrospective analyses of data from patients who had received carboplatin/paclitaxel, in order to identify prognostic variables affecting OS and progession-free survival (PFS), and also to determine the contribution of second-line and subsequent treatment to prolongation of OS.

Patients and Methods

Patients. This retrospective study recruited patients with NSCLC who had received chemotherapy at the Thoracic Oncology Division, Shizuoka Cancer Center, Japan, between October 2002 and September 2005. Patients met all of the following criteria:[1] clinical stage IIIB or IV;[2] patients were administered carboplatin area under the curve (AUC) 6 + paclitaxel 200 mg/m^2 as first-line chemotherapy; and[3] performance status (PS) 0 or 1.

Target patients were identified in our electronically controlled clinical database and the following information extracted from their data:[1] patient demographics at the start of first-line chemotherapy (age, gender, smoking history, histology, stage);[2] objective tumor response;[3] time to disease progression;[4] OS;

[3]To whom correspondence should be addressed. E-mail: n.yamamoto@scchr.jp

doi: 10.1111/j.1349-7006.2006.00379.x

and second-line and subsequent chemotherapy regimens.[5] The tumor response was evaluated according to Response Evaluation Criteria in Solid Tumors (RECIST) using existing images and graded as complete response, partial response, stable disease, progressive disease or not evaluable.

Treatment. Patients received carboplatin and paclitaxel as first-line chemotherapy. Patients received paclitaxel 200 mg/m^2 as a 3-h intravenous infusion, followed by carboplatin AUC 6 (Calvert's setting) as a 1-h infusion on Day 1. Courses of treatment were repeated every 3 or 4 weeks for 4–6 cycles, until disease progression or severe toxicity. When a patient developed National Cancer Institute Common Toxicity Criteria (NCI-CTC) grade 3 non-hematological toxicity (except nausea and anorexia) after the start of treatment, the dose was reduced to carboplatin AUC 5 + paclitaxel 150 mg/m^2.

Statistical analysis. Kaplan-Meier plots were prepared for OS and PFS and median values were calculated. OS was measured from the first day of first-line treatment to the day of death or the day last seen alive (cut-off). PFS was measured from the first day of first-line treatment to the earliest observation of documented progressive disease, or the day of death if the patient died before observation of progressive disease. Univariate and multivariate analyses were performed for OS and PFS stratified by baseline factors. To identify factors influencing PFS and OS, multivariate analysis was performed with covariates including disease stage (IIIB versus IV), histology (adenocarcinoma versus other), smoking history (non-smoker versus smoker), gender (female versus male) and PS (0 versus 1). Multivariate analysis was performed by the stepwise regression method using a Cox proportional hazards model. To evaluate potential interaction between clinical variables such as smoking history or histology and EGFR-TKI treatment, patients who received second-line therapy were included in subsequent exploratory Cox analysis in which non-smokers and adnocarcinoma patients were divided by EGFR-TKI treatment, with smokers and nonadnocarcinoma patients set as references, respectively. Statistical analyses for this study were conducted using the Stat View software statistical tool.

Results

Patient characteristics. In total, 98 patients met the eligibility criteria and their demographic data are presented in Table 1. The majority of patients were male (64%), had a smoking history (69%), adenocarcinoma histology (76%), stage IV disease (70%) and PS 0 (57%). The median duration of first-line carboplatin/paclitaxel therapy was 3 cycles (range, 1–6 cycles). The median follow-up time was 24.8 months (range: 4.2–43.9). 57 patients died. 41 patients were still alive.

Table 1. Patient demographics ($n = 98$)

Gender *n* (%)	
Male	63 (64)
Female	35 (36)
Median (range) age, years	61 (34–78)
ECOG PS, *n* (%)	
0	56 (57)
1	42 (43)
Smoking history, *n* (%)	
Smoker	68 (69)
Non-smoker	30 (31)
Histology, *n* (%)	
Adenocarcinoma	74 (76)
Other	24 (24)
Stage, *n* (%)	
IIIB	29 (30)
IV	69 (70)

ECOG, European Cooperative Oncology Group; PS, performance status.

Table 2. Best overall objective response, *n* (%)

	Total population ($n = 98$)	By histology	
		Adenocarcinoma ($n = 74$)	Other ($n = 24$)
Partial response	20 (20)	15 (20)	5 (21)
Stable disease	53 (54)	42 (57)	11 (46)
Progressive disease	25 (26)	17 (23)	8 (33)

Efficacy. The overall response rate to first-line carboplatin/paclitaxel therapy was 20% (20/98), with outcomes similar in patients with adenocarcinoma and other histological subtypes (20% versus 21%, respectively) (Table 2). In the overall population, median PFS was 4.8 months and median OS 16.5 months, with a 1-year survival rate of 64%.

For PFS, only disease stage was a significant prognostic factor (Table 3). For OS, histology, smoking history and PS were significant prognostic factors (Table 3).

Multivariate analyses assessing the effects of histology and smoking history on PFS and OS were performed. No significant difference was observed for PFS between adenocarcinoma versus other histology ($P = 0.40$; Fig. 1) or non-smokers versus smokers ($P = 0.22$; Fig. 2). In contrast, OS differed significantly between adenocarcinoma versus other histology ($P = 0.0017$)

Table 3. Efficacy among patient subgroups: Cox regression analysis

Factor	Variable	PFS *P*-value HR (95% CI)	OS *P*-value HR (95% CI)
Histology	Adenocarcinoma versus other	0.2045 –	0.0020 0.410 (0.233–0.723)
Smoking	Non-smoker versus smoker	0.1351 –	<0.0001 0.222 (0.109–0.450)
Gender	Female versus male	0.2206 –	0.2691 –
PS	0 versus 1	0.9575 –	0.0109 0.499 (0.292–0.852)
Stage	IIIB versus IV	0.0074 0.536 (0.339–0.847)	0.2024 –

PFS, progression-free survival; OS, overall survival; HR, hazard ratio; CI, confidence interval; NS, not significant; PS, performance status.